Neutron stars in the lab

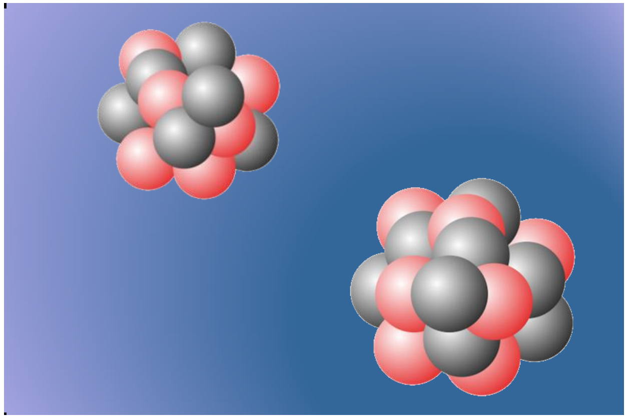

1 fm

10^{18} fm

J. Benlliure

IGFAE course on neutron star physics

Nov. 15th-19th 2021

Matter at high pressure

Neutron stars and terrestrial laboratories.

The highest pressure in terrestrial labs.

nature

Explore content ⌄ About the journal ⌄ Publish with us ⌄

nature > articles > article

Article | Published: 27 January 2021

Metastability of diamond ramp-compressed to 2 terapascals

A. Lazicki, D. McGonegle, J. R. Rygg, D. G. Braun, D. C. Swift, M. G. Gorman, R. F. Smith, P. G. Heigh… A. Higginbotham, M. J. Suggit, D. E. Fratanduono, F. Coppari, C. E. Wehrenberg, R. G. Kraus, D. Erskine… Bernier, J. M. McNaney, R. E. Rudd, G. W. Collins, J. H. Eggert & J. S. Wark

Nature 589, 532–535 (2021) | Cite this article

Abstract

Carbon is the fourth-most prevalent element in the Universe and essential for all known life. In the elemental form it is found in multiple allotropes, including graphite, diamond and fullerenes, and it has long been predicted that even more structures can exist at pressures greater than those at Earth's core[1,2,3]. Several phases have been predicted to exist in the multi-terapascal regime, which is important for accurate modelling of the interiors of carbon-rich exoplanets[4,5]. By compressing solid carbon to 2 terapascals (20 million atmospheres; more than five times the pressure at Earth's core) using ramp-shaped laser pulses and simultaneously measuring nanosecond-duration time-resolved X-ray diffraction,

Lawrence Livermore National Laboratory

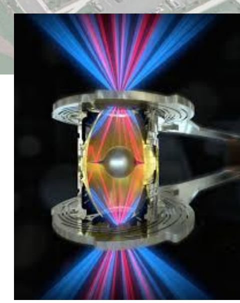

16 laser beams of 500 TW/cm^2 impinging simultaneously on a sample.

Estimated pressure in neutron stars.

$$P = H\rho g \qquad g = GM / R^2 \approx 6{,}8 \cdot 10^{13}\ m/s^2$$

ρ (g/cm³)	H (m)	P (Pa)
5 10^{-3}	1,4 10^{-2}	4,7 10^{12}
1	8,2 10^{-2}	5,5 10^{15}
10^{3}	8,2 10^{-1}	5,5 10^{19}
10^{7}	1,7 10^{1}	1,2 10^{25}
10^{11}	3,8 10^{2}	2,5 10^{30}
10^{15}	8,2 10^{3}	5,5 10^{35}

Only relativistic heavy-ion collisions produces similar pressures(density) values at microscopic level (ρ_o~ 0,17 fm^{-3} ~ 2.2 10^{14} g/cm^3).

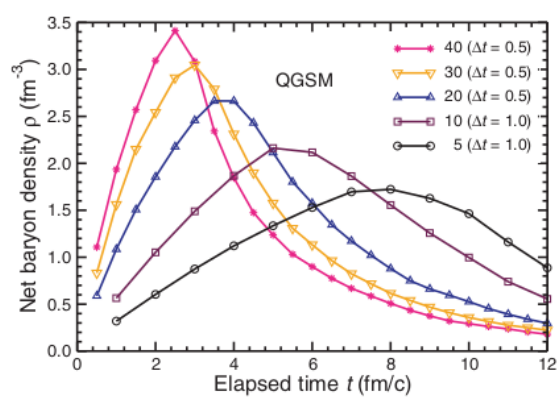

Layout

- ✓ Basic concepts on neutron stars.
- ✓ Outer crust in non-accreting neutron stars.
- ✓ Inner crust in neutron stars.
- ✓ Neutron star core.
- ✓ Facilities.
- ✓ Future perspectives.

Basic concepts on neutron stars

Structure and composition

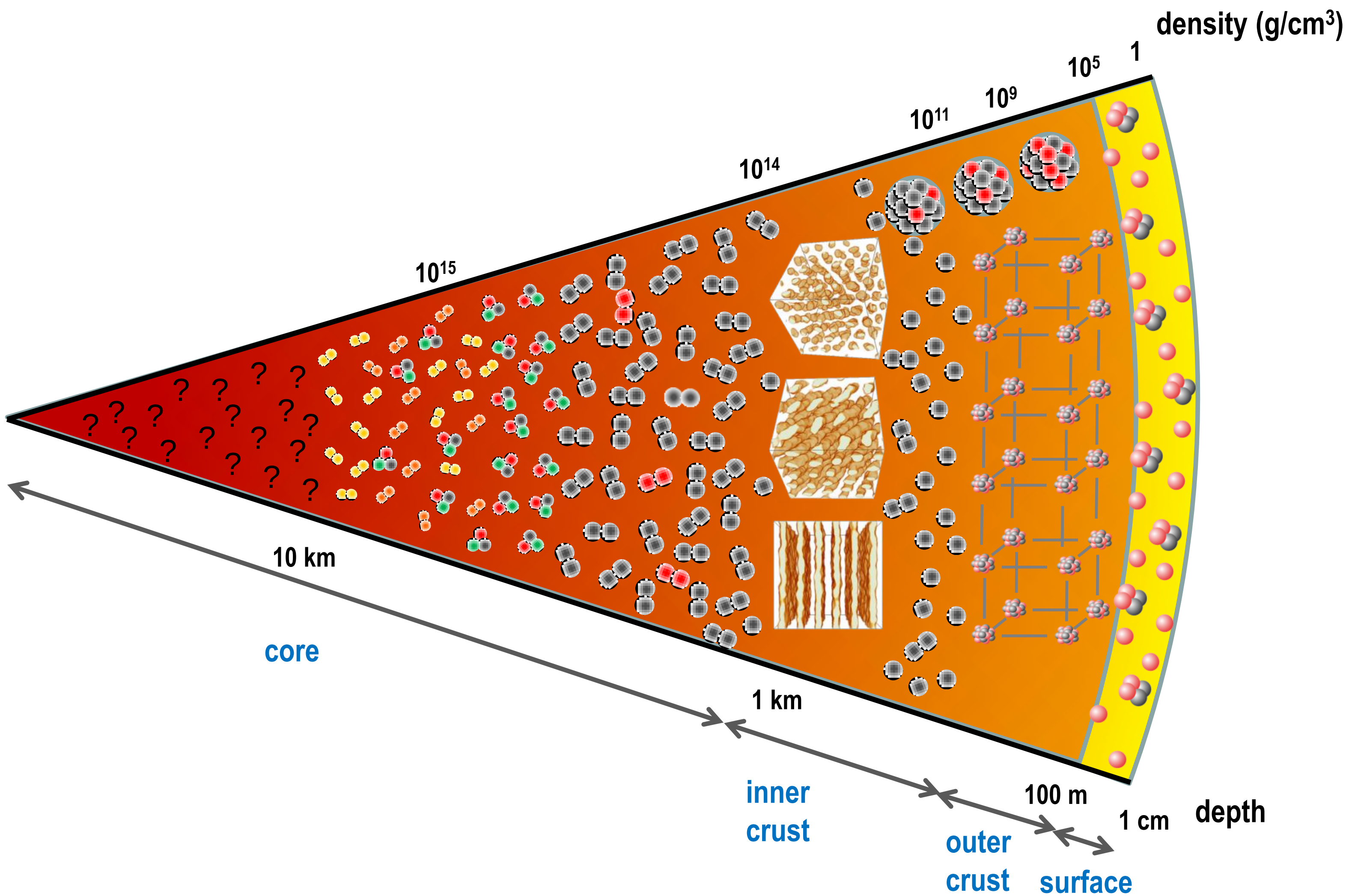

Some basic concepts on neutron stars

Modelling: assumptions and physical laws

- **Hydrostatic equilibrium** (Tolman, Oppenheimer and Volkoff equations).

$$\frac{dP}{dr} = -G\frac{\varepsilon m}{r^2}\left(1+\frac{P}{\varepsilon}\right)\left(1+\frac{4\pi \Pr^3}{m}\right)\left(1-\frac{2Gm}{r}\right)^{-1}$$

$$\frac{dm}{dr} = 4\pi r^2 \varepsilon$$

- **Thermodynamical equilibrium** (equation of state).

$$dE = dQ - PdV \rightarrow P(T=0) = n^2\frac{d(\varepsilon/n)}{dn} = n\frac{d\varepsilon}{dn} - \varepsilon = n\mu - \varepsilon$$

μ: chemical potential.

n: particle number density.

ε: total energy density.

ionized matter: $\varepsilon = nm_N + \varepsilon_F^e$

baryonic matter: $\varepsilon = n_n m_n + n_p m_p + (n_n + n_p)E + \varepsilon_e + \varepsilon_\mu$

ε_F : Fermi energy.

E: energy per baryon.

- **β-equilibrium**.

$$\mu_i = b_i\mu_n - q_i\mu_e$$

b_i and q_i are the baryon number and charge of species *i*.

- **Charge neutrality**.

$$\sum_i n_i q_i = 0$$

Some basic concepts on neutron stars

Modelling: matter transformation with pressure

- **Ionization** ($\rho \sim 1 - 10^5$ *g/cm³*).

Distance between atoms d_i: $\frac{4\pi}{3} d_i^3 n = 1 \quad n = \rho / A m_N$ $\quad d_i = d_Z \downarrow$

Atomic radius a_Z: $a_Z = \frac{1}{Z} \frac{\hbar}{\alpha m_e c} \quad \hbar / \alpha m_e c = 0.53 \cdot 10^{-10}\ m \quad \rho = \frac{3 A m_N}{4\pi} \left(\frac{\alpha m_e c Z}{\hbar} \right)^3$

ion	ρ (g/cm³)	H (m)
H	1,7	9,7 10^{-2}
^{4}He	5,4 10^1	3,1 10^{-1}
^{12}C	4,4 10^3	1,3
^{56}Fe	1,7 10^6	9,7

- **Electron degeneracy** ($\rho \sim 10^5 - 10^7$ *g/cm³*).

Fermi energy: $\varepsilon_F = \frac{\hbar^2 (3\pi^2 n_e)^{2/3}}{2 m_e} \quad n_e = \rho Y_e / m_N \quad \varepsilon_F = E_T \downarrow$

Thermal energy: $E_T = k_B T \quad \rho = \frac{m_N}{3\pi^2 Y_e} \left(\frac{2 m_e k_B T}{\hbar^2} \right)^{3/2}$

T(K)	ρ (g/cm³)	H (m)
5 10^8	1,3 10^5	4,2
1 10^9	3,9 10^5	5,9
5 10^9	4,3 10^6	13
1 10^{10}	1,2 10^7	19
5 10^{10}	1,4 10^8	42

- **Ion matter configuration** ($\rho > 10^6$ *g/cm³* ^{56}Fe solid)

Coulomb energy:

Thermal energy:

$$\Gamma = \frac{E_{Coul}}{E_T} = \frac{1}{4\pi\varepsilon_o} \frac{Z^2 e^2}{d_i k_B T}$$

Γ << 1 gas

Γ < 1 liquid

Γ >1 solid

Γ(^{56}Fe)	ρ (g/cm³)	H (m)
0,1	5,9 10^1	0,3
1	5,9 10^4	3,2
5	7,4 10^6	16
10	5,9 10^7	32

Some basic concepts on neutron stars

Modelling: matter transformation with pressure

- **Neutronization** ($\rho \sim 2\ 10^7\ g/cm^3$).

$e^- + p \rightarrow n + \nu \qquad \varepsilon_F > (m_n - m_p)c^2 = 1{,}3$ MeV

$$n_e = \frac{1}{3\pi^2}\left(\frac{p_F}{\hbar}\right)^3 \approx 7 \cdot 10^{30}\ cm^{-3} \qquad \rho = \frac{n_e m_N}{Y_e} \approx 2 \cdot 10^7\ g/cm^3$$

- **Neutron drip** ($\rho \sim 4\ 10^{11}\ g/cm^3$).

$$\mu_n' = \mu_n - m_n c^2 = \frac{d\varepsilon}{dn} - m_n c^2$$

μ' < 0 neutron bound

μ' ≥ 0 neutron unbound

$$\delta_{drip}(\mu' = 0) = \sqrt{1 - E_{vol}/E_{sym}} - 1 = 0{,}225$$

$$B(A,Z) = \varepsilon - Am_n c^2 \rightarrow \varepsilon \approx A(E_{vol} + E_{sym}\delta^2) \quad \delta = (N - Z)/A$$

$$p + e^- \leftrightarrow n + \nu_e \Rightarrow \mu_e = \mu_n - \mu_p \approx 4E_{sym}\delta$$

$$\rho(\delta_{drip}) \approx 4 \cdot 10^{11}\ g/cm^3$$

relativistic electrons $\mu_e \approx \varepsilon_F \approx p_F c = \hbar c(3\pi^2 n_e)^{1/3} \qquad n_e = \rho Y_e / m_N$

- **Nuclei decomposition** ($\rho \sim 10^{14}\ g/cm^3$).

- **Muonic and strange matter** ($\rho \sim 5\ 10^{14}\ g/cm^3$).

$$n + e^- \rightarrow \Sigma^- + \nu_e \qquad \mu_\Sigma = \mu_n + \mu_e - \mu_\nu$$

$$n + n \rightarrow n + \Lambda \qquad \mu_\Lambda = \mu_n$$

Some basic concepts on neutron stars

Equation of state for neutron stars

The equation of state determines important macroscopic properties of the star as its mass and radius, but also the boundaries between different states of matter, or the cooling mechanism of nascent neutron stars.

$$dE = dQ - PdV \rightarrow P(T=0) = n^2 \frac{d(\varepsilon / n)}{dn} = n \frac{d\varepsilon}{dn} - \varepsilon = n\mu - \varepsilon$$

At densities below the neutron-drip value (ρ~*4 10^{11} g/cm^3, H < 1 km*) matter pressure is dominated by the relativistic electron gas and the corresponding equation of state can be obtained using the **Fermi gas** model.

$$\varepsilon = nm_N + \varepsilon_F^e$$

Above the neutron-drip density (ρ~*4 10^{11} g/cm^3, H > 1 km*) matter pressure is dominated by the energy density of neutrons and the general **energy density for lepton/baryon matter** is:

$$\varepsilon = n_n m_n + n_p m_p + (n_n + n_p)E + \varepsilon_e + \varepsilon_\mu$$

where *E* is the energy per baryon as function of the density (ρ) and isospin asymmetry (δ).

Some basic concepts on neutron stars

Scenarios

The composition and structure of a neutron star is at first order defined by its mass, this composition can however change in interacting stars like accreting neutron stars or neutron star mergers.

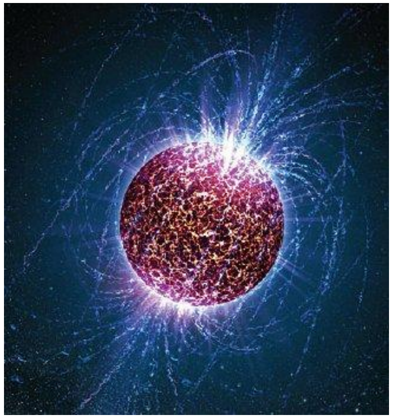

Nonaccreting neutron stars

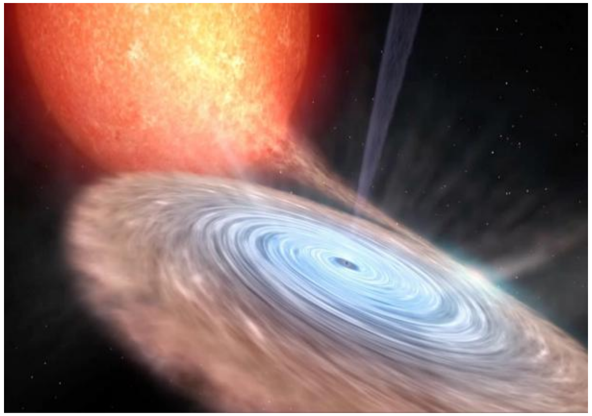

Accreting neutron stars

Neutron star mergers

Outer crust in nonaccreting neutron stars

Coulomb crystals

Above 10^5 g/cm^3 matter is completely ionized and electrons degenerated. The pressure of the electron Fermi gas balance gravitation, but the composition and structure of the star is governed by β-equilibrium and the competition between thermal energy and Coulomb attraction.

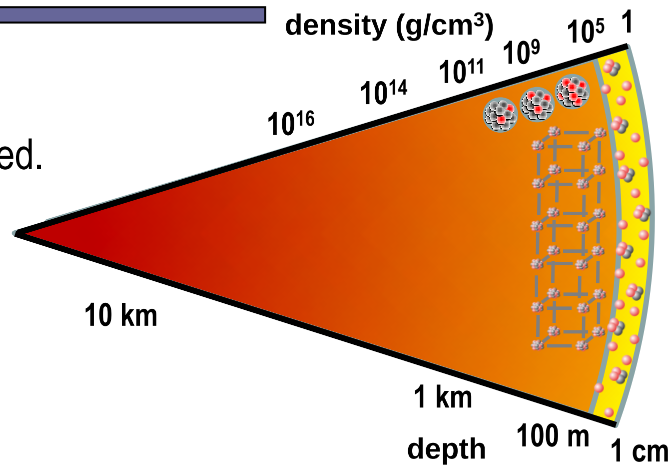

$$\Gamma = \frac{E_C}{E_T} = \frac{1}{4\pi\varepsilon_o}\frac{Z^2 e^2}{d_i k_B T} \qquad \frac{4\pi}{3} d_i n_N = 1 \qquad n_N = \frac{\rho}{A m_N}$$

For $\rho > 10^6$ *g/cm*^{3} and $T \sim 10^9$ K, $\Gamma > 1$ and ions form a solid Coulomb crystal whose ground state can be obtained minimizing the energy density assuming a single nuclear species for a given baryon density n_b.

$$\varepsilon_{tot} = n_N E(A,Z) + \varepsilon_e(n_e) + \varepsilon_L(n_e)$$

$$n_N = n_b / A \qquad n_e = n_b Z / A$$

n_N: number density of nuclei

$E(A,Z)$: the energy of the nuclear species

ε_e: electron kinetic energy density

ε_L: lattice energy density

For a degenerate Fermi gas: $\varepsilon_e = \frac{m_e^4 c^5}{8\pi^2\hbar^3}\left[x_r\left(2x_r^2+1\right)\sqrt{x_r^2+1} - \ln\left(x_r + \sqrt{x_r^2+1}\right)\right] \quad x_r = p_{F,e}/m_e c$

The lattice energy density can be estimated, assuming spherical atoms whose radius is defined by the stellar density, as the density of nuclei times the Coulomb energy of one such sphere.

$$\varepsilon_L = -\frac{9}{10}\left(\frac{4\pi}{3}\right)^{1/3} Z^{2/3} e^2 n_e^{4/3}$$

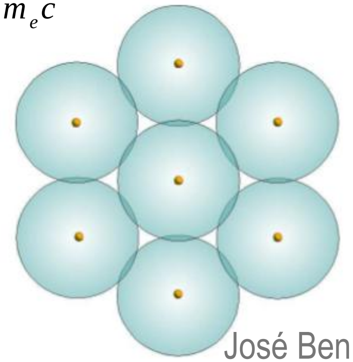

Outer crust in nonaccreting neutron stars

Coulomb crystals

The minimum energy density corresponds to a **body-centered cubic lattice made of ^{56}Fe ions**. Increasing density, the minimization of the energy density *E(N,Z),* and β-equilibrium transform the ion species of the lattice in heavier and more neutron-rich ones, until the neutron drip-line is reached.

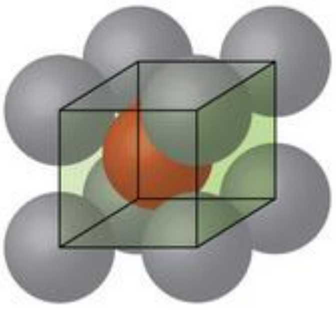

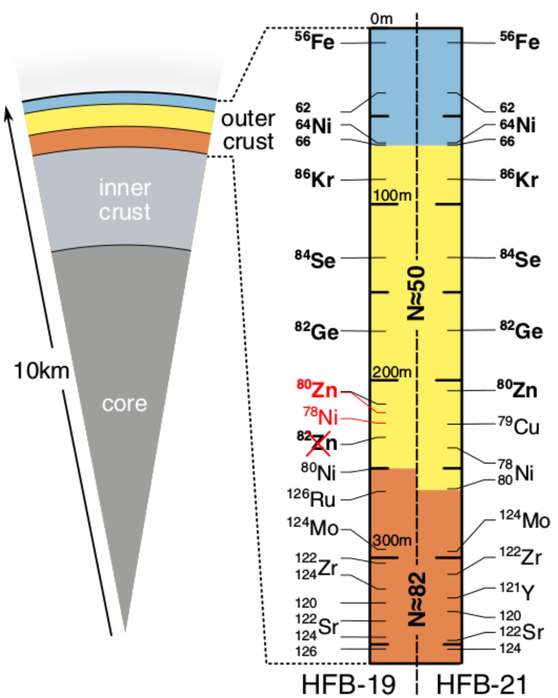

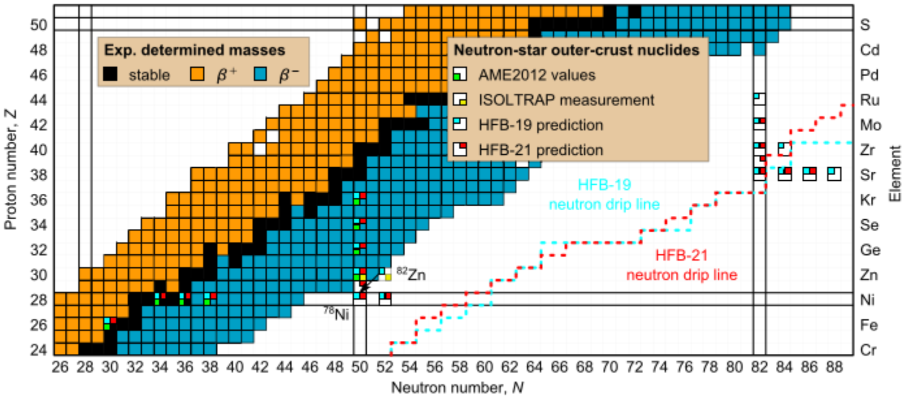

Nuclear models do not have the accuracy required to predict the sequence of nuclear species in the outer crust, neither the position of the neutron drip-line.

Masses should be measured.

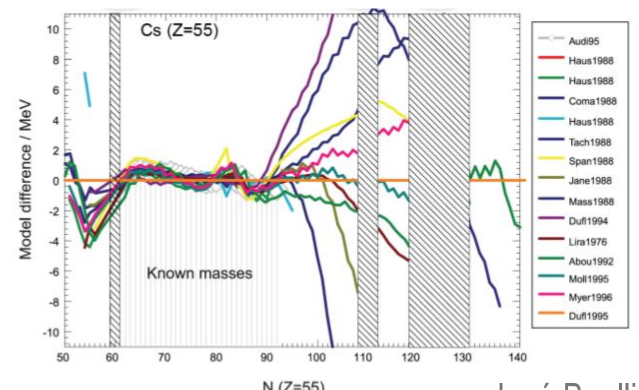

Outer crust in nonaccreting neutron stars

Mass measurements of neutron-rich nuclei

To determine the nuclei that constitute the outer crust of neutron stars one needs facilities producing neutron-rich nuclei along N=28 and N=50 and experimental techniques providing accurate measurements.

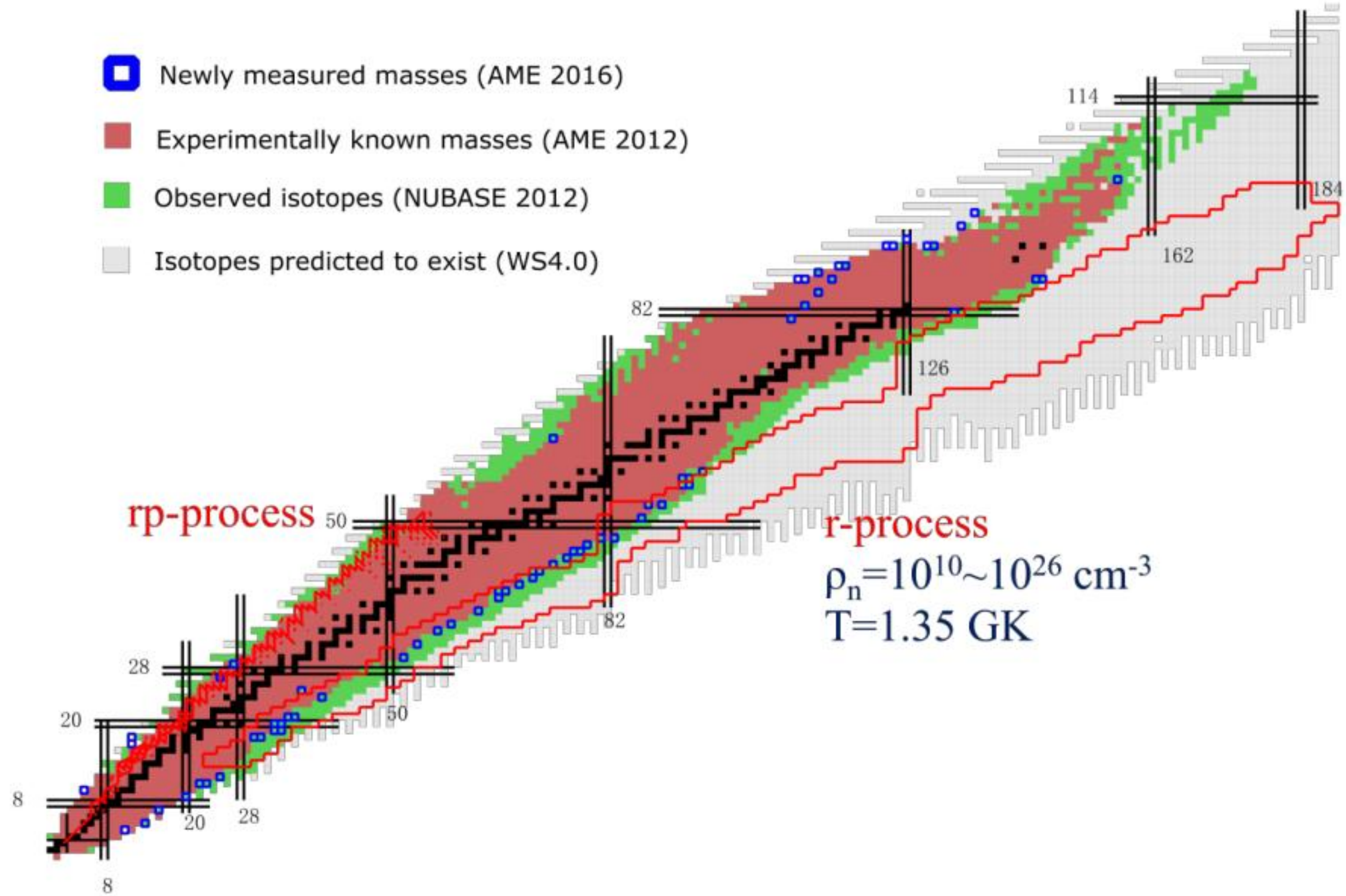

Outer crust in nonaccreting neutron stars

Mass measurements of neutron-rich nuclei

Two techniques for the production of nuclei far from stability.

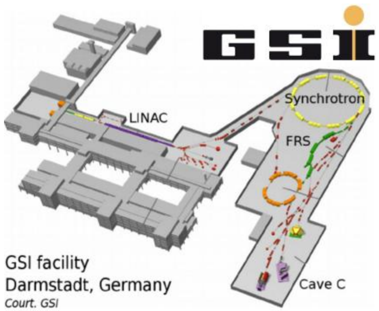

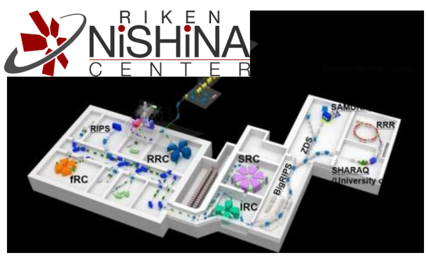

Facility for Rare Isotope Beams at Michigan State University

FAIR

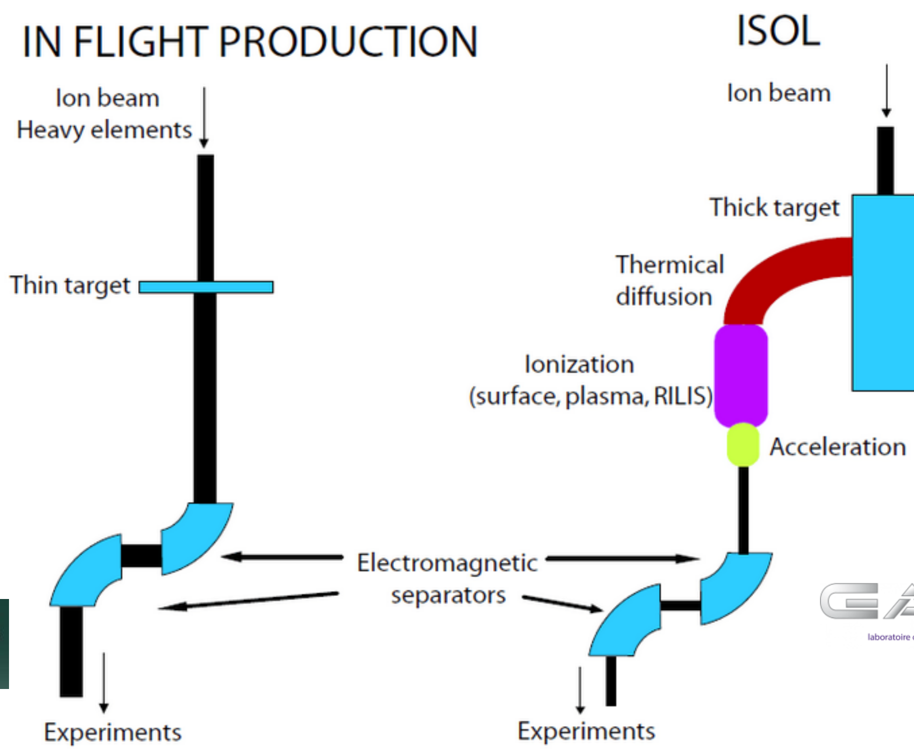

High-energy exotic beams, GeVs

Low-energy exotic beams, MeVs

ISOLDE CERN

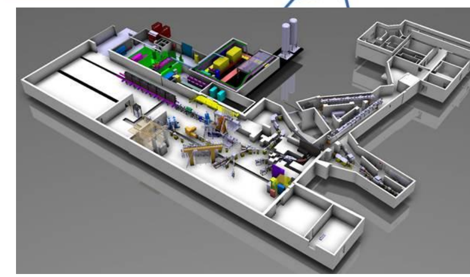

TRIUMF

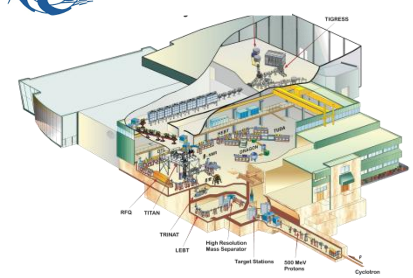

GANIL spiral2

SPES exotic beams for science

EURISOL

Outer crust in nonaccreting neutron stars

Mass measurements of neutron-rich nuclei

Most accurate measurements of nuclear masses using ion traps, $\Delta m/m \sim 10^{-10}$ (few hundred eV).

Measurement of the cyclotron frequency of ions trap by a uniform magnetic field and a quadrupolar electric field.

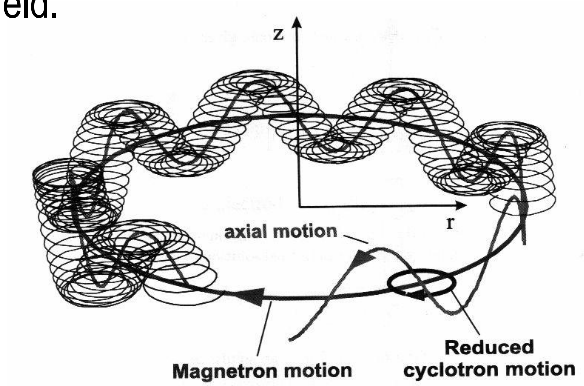

$$\omega_c = (q/m)B = \omega_+ + \omega_- = \sqrt{\omega_+^2 + \omega_-^2 + \omega_z^2}$$

A radio-frequency (ω_r) acting on the electrodes that generate the quadrupolar electric field ,couple the three different movements. When $\omega_r = \omega_c$ the axial energy is maximal and the time of flight (ToF) of the ions, after the trap opening, minimum.

ISOL-TRAP @ Isolde/CERN

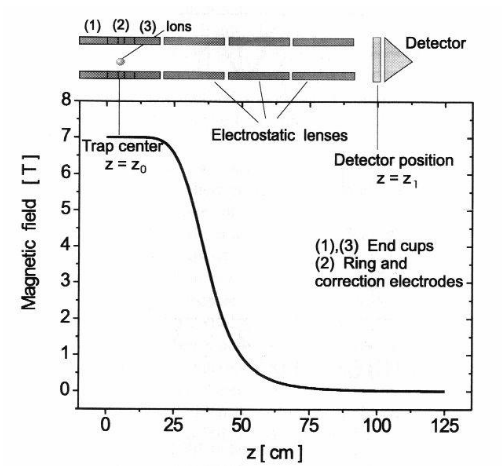

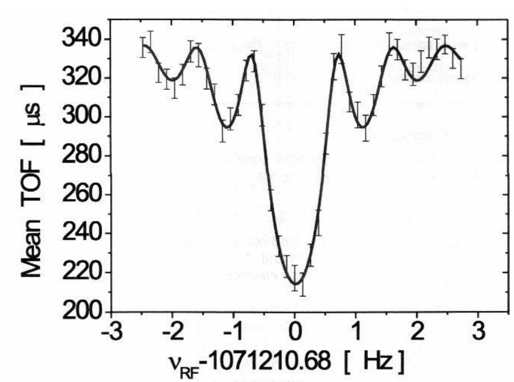

Outer crust in nonaccreting neutron stars

Mass measurements at ISOL-TRAP @ Isolde-CERN

Precise measurements of the mass of ^{82}Zn, provided a new composition profile of the neutron-star crust.

PRL **110,** 041101 (2013) PHYSICAL REVIEW LETTERS week ending 25 JANUARY 2013

Plumbing Neutron Stars to New Depths with the Binding Energy of the Exotic Nuclide ^{82}Zn

R. N. Wolf,[1,*] D. Beck,[2] K. Blaum,[3] Ch. Böhm,[3] Ch. Borgmann,[3] M. Breitenfeldt,[4] N. Chamel,[5] S. Goriely,[5] F. Herfurth,[2] M. Kowalska,[6] S. Kreim,[3,6] D. Lunney,[7] V. Manea,[7] E. Minaya Ramirez,[2,8] S. Naimi,[7,9] D. Neidherr,[2,3] M. Rosenbusch,[1] L. Schweikhard,[1] J. Stanja,[10] F. Wienholtz,[1] and K. Zuber[10]

[1]*Institut für Physik, Ernst-Moritz-Arndt Universität Greifswald, 17487 Greifswald, Germany*
[2]*GSI Helmholtzzentrum für Schwerionenforschung GmbH, Planckstraße 1, 64291 Darmstadt, Germany*
[3]*Max-Planck-Institut für Kernphysik, Saupfercheckweg 1, 69117 Heidelberg, Germany*
[4]*Instituut voor Kern- en Stralingsfysica, KU Leuven, Celestijnenlaan 200d, B-3001 Heverlee, Belgium*
[5]*Institut d'Astronomie et d'Astrophysique, CP-226, Université Libre de Bruxelles, 1050 Brussels, Belgium*
[6]*CERN, 1211 Geneva 23, Switzerland*
[7]*CSNSM-IN2P3-CNRS, Université Paris-Sud, 91405 Orsay, France*
[8]*Helmholtz-Institut Mainz, 55099 Mainz, Germany*
[9]*RIKEN Nishina Center for Accelerator-based Science, RIKEN, 2-1 Hirosawa, Wako-shi, Saitama 351-0198, Japan*
[10]*Institut für Kern- und Teilchenphysik, Technische Universität Dresden, 01069 Dresden, Germany*
(Received 28 October 2012; published 22 January 2013)

Modeling the composition of neutron-star crusts depends strongly on binding energies of neutron-rich nuclides near the $N = 50$ and $N = 82$ shell closures. Using a recent development of time-of-flight mass spectrometry for on-line purification of radioactive ion beams to access more exotic species, we have determined for the first time the mass of ^{82}Zn with the ISOLTRAP setup at the ISOLDE-CERN facility. With a robust neutron-star model based on nuclear energy-density-functional theory, we solve the general relativistic Tolman-Oppenheimer-Volkoff equations and calculate the neutron-star crust composition based on the new experimental mass. The composition profile is not only altered but now constrained by experimental data deeper into the crust than before.

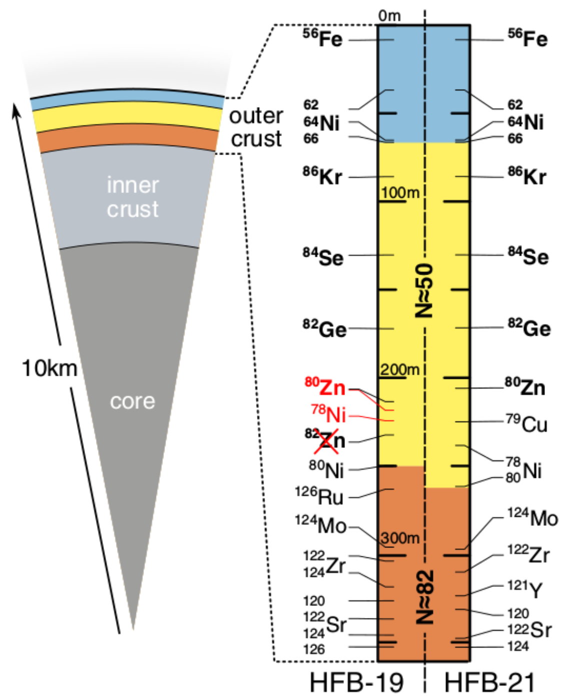

The detailed composition of deeper layers will require new exotic beam facilities presently under construction.

Inner crust in neutron stars

Structure and composition

Electron capture produces more and more neutron-rich nuclei until the neutron drip-line is reached. At this point the Fermi level for neutrons equals the rest mass of the neutron, and the ground state for further electron captures consist on nuclei at the drip-line and free neutrons.

$$ {}^{A}_{Z}X + e^{-} \rightarrow {}^{A-1}_{Z-1}Y + n + \nu_e $$

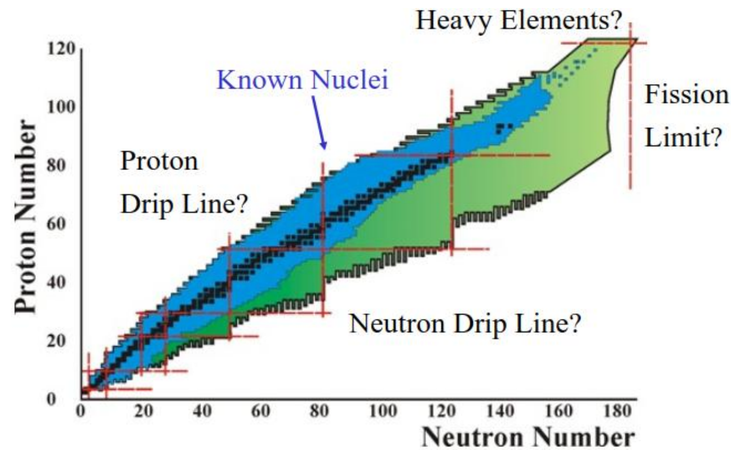

Using the leading terms from the nuclear liquid-drop model and the definition of drip-line:

$$ S_n^{drip} = B(A,Z) - B(A-1,Z) \geq 0 $$

$$ B(A,Z) \approx A(E_{vol} + E_{sym}\delta^2) \qquad \delta = (N-Z)/A $$

$$ \delta_{drip} = \sqrt{1 - E_{vol}/E_{sym}} - 1 \approx 0{,}225 \qquad \begin{cases} E_{vol} \approx -16\ MeV \\ E_{sym} \approx 32\ MeV \end{cases} $$

The density at which neutron drip, and the inner crust, starts, can be obtained from the β-equilibrium condition:

$$ \mu_e = \mu_Y - \mu_X - \mu_n \approx 4E_{sym}\delta $$

$$ \mu_e \approx 5.16\left(\rho_9 Z/A\right)^{1/3} MeV $$

$$ \rho_{drip} \approx 2\cdot 10^{11}\ g/cm^3 $$

State-of-the-art model calculations predict a density value for the neutron drip around 4 10^{11} g/cm^3.

Inner crust in neutron stars

Structure and composition

The inner crust of neutron stars corresponds to the density range between neutron drip (ρ_{drip}~*4 10^{11} g/cm^3*) and nuclei decomposition (ρ_{core}~*10^{14} g/cm^3* ~ ρ_0) . In this region the solid **Coulomb lattice** coexists with a **neutron fluid**. The contribution of these free neutrons to the internal pressure of the star increases with density, reaching *80%* at *10^{13} g/cm^3*.

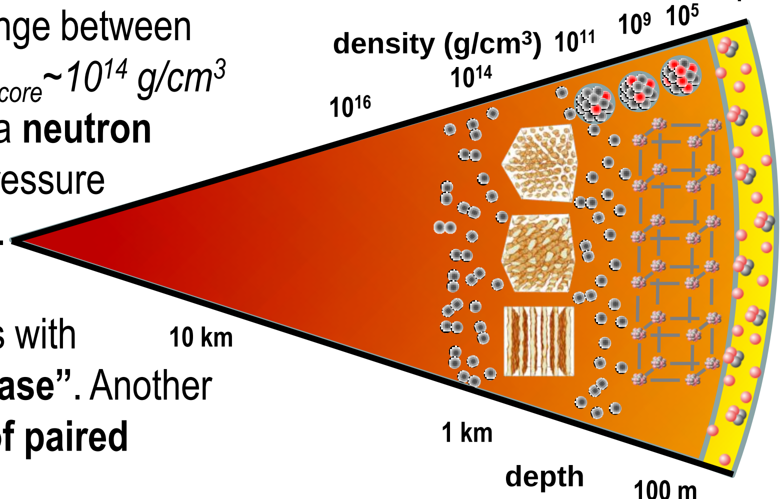

Several models predict the appearance of clusters of neutrons with characteristic geometrical configurations known as **"pasta phase"**. Another interesting prediction is the formation of a **superfluid phase of paired neutrons** and a **superconducting phase of paired protons**.

This kind of matter can not be produced in terrestrial experiments. However, the main ingredient in model descriptions, the **equation of state** of asymmetric nuclear matter at densities around saturation density, can be investigated in experiments at facilities producing beams of nuclei far from stability.

Some of the key inputs to constraint this equation of state are the isospin and density dependence of the **symmetry energy**, and the role of **NN correlations** in the nucleon-nucleon interaction that affects the superfluid neutron and the superconducting proton phases.

Inner crust in neutron stars

Equation of state of asymmetric nuclear matter

The equation of state of asymmetric nuclear matter as function of density (ρ) and isospin asymmetry (δ) can be expressed in terms of the energy per nucleon that, using the parabolic approximation, can be written as:

$$E(\rho,\delta) = E_o + \frac{1}{2}K_o x^2 + \left(S_o + Lx + \frac{1}{2}K_{sym} x^2 \right)\delta^2$$

$$x = \frac{\rho - \rho_o}{3\rho_o} \qquad \delta = \frac{\rho_n - \rho_p}{\rho_n + \rho_p}$$

where the isoscalar parameters (*E_o=-16 MeV, K_o=240±20 MeV*) are well known, in contrast to the isovector ones, defining the so called symmetry energy.

$$E_{sym}(\rho) = E_{PNM}(\rho) - E_{SM}(\rho) = S_o + Lx + \frac{1}{2}K_{sym} x^2$$

The isovector parameters (*S_o, L, and K_{sym}*) play a major role in the neutron star EOS (transition to neutron drip, mass of the star, …). During the last decade a number of terrestrial experiments involving isospin asymmetric nuclei have tried to constraint the values of those parameters to identify realistic nuclear forces providing accurate EOS.

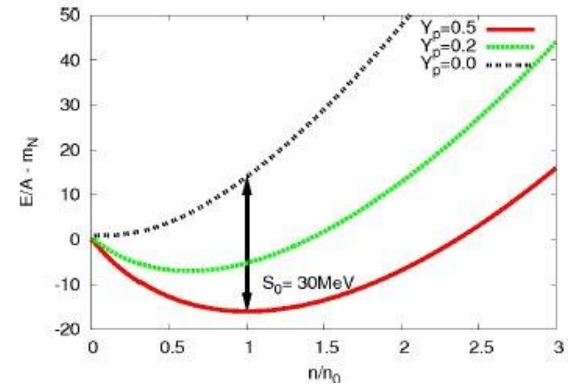

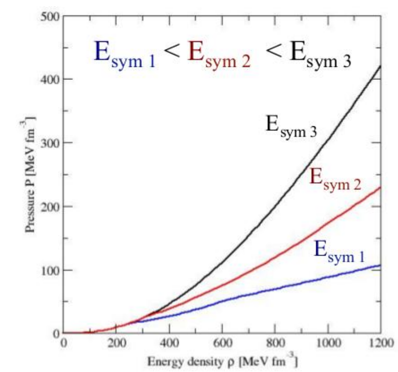

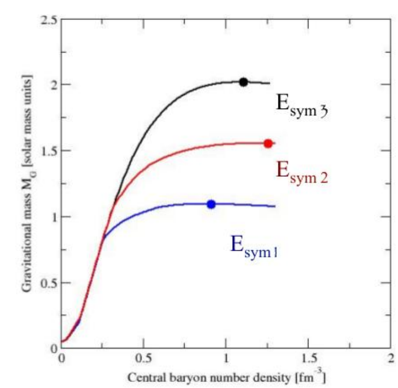

Constraining the symmetry energy at $\rho \leq \rho_o$

Nuclear masses

The more than 2000 existing measurements of nuclear masses provide the easiest and more statistically significant method to constrain the symmetry energy around saturation density.

$$B(N,Z) = a_{vol}A - a_{surf}A^{2/3} - a_C\frac{Z^2}{A^{1/3}} - a_{asym}\frac{(N-Z)^2}{A} + a_{pairing}$$

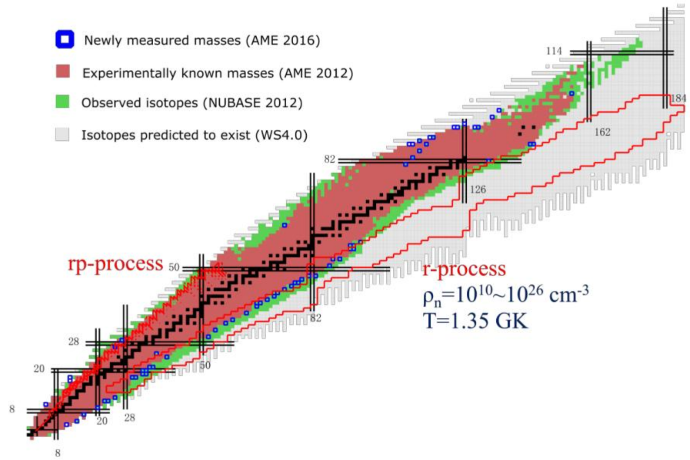

The basic liquid-drop model for nuclear binding energy already provides direct input on the value of the symmetry energy at saturation density ($a_{asym} = S_o \sim 32\ MeV$).

The fitting of advanced nuclear interaction parameters to measured nuclear masses using microscopic models has provide an accurate value of the symmetry energy at saturation density ($S_o = 30.5 - 31.2\ \ MeV$) and a good estimate of the density slope parameter ($L = 41{,}5 - 56.6\ MeV$).

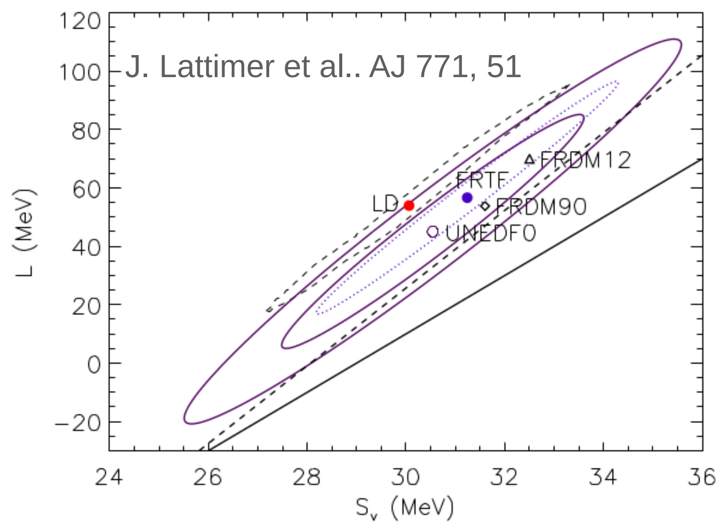

Constraining the symmetry energy at $\rho \leq \rho_o$

Neutron skin thickness of neutron-rich nuclei

The neutron skin thickness of heavy nuclei have been shown as one of the most sensitive terrestrial probes of the density slope of the symmetry energy *(L)* at subsaturation densities.

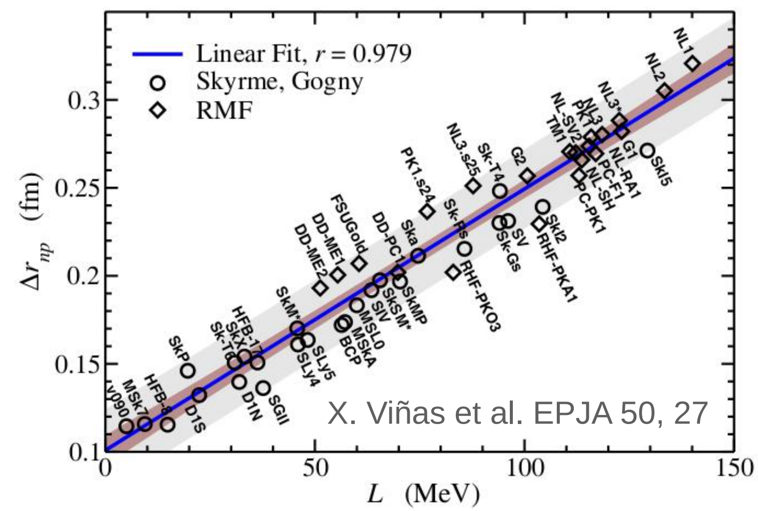

The neutron skin thickness is the difference in root-mean-square neutron and proton nuclear radii.

$$\Delta r_{np} = \langle r^2 \rangle_n^{1/2} - \langle r^2 \rangle_p^{1/2}$$

Proton nuclear radii can be accurately determine using elastic electron scattering (up to now only with stable nuclei).

$$\frac{d\sigma}{d\Omega} = \left| F_{ch}^{A}(q) \right|^2 \frac{d\sigma}{d\Omega}_{Mott} \qquad F_{ch}^{A}(q) \Leftrightarrow \rho_{ch}^{A}(r)$$

$$F_{ch}^{A}(q) \cdot F_p(q) \Leftrightarrow \rho_p(r)$$

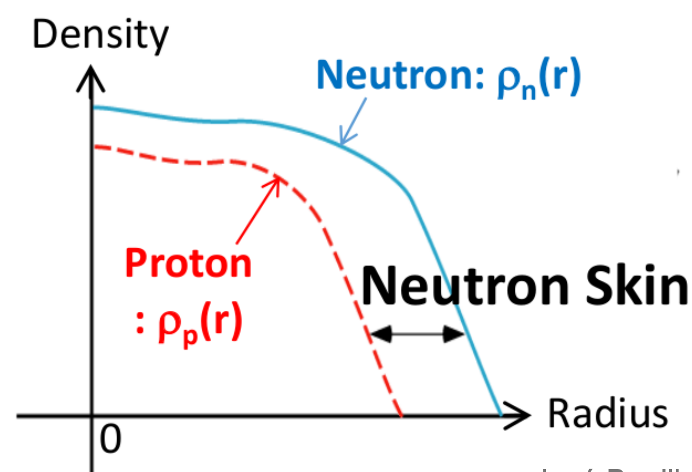

Neutron nuclear radii require hadronic probes that produce larger uncertainties. Some techniques:

- Proton elastic scattering.
- Anti-protonic atoms.
- Electric dipole dipolarizability.
- Parity violating electron scattering.

USC
UNIVERSIDADE DE SANTIAGO DE COMPOSTELA

Constraining the symmetry energy at $\rho \leq \rho_o$

Neutron skin thickness of neutron-rich nuclei

Elastic proton scattering.

Precise measurements of the angular distributions of elastically scattered protons on different stable tin isotopes at 300 MeV performed at at RCNP (Osaka) provided an accurate determination of the neutron skin thickness using previously measured proton radii.

Those measurements have been used to provide stringent constraints on the density slope parameter (*L*) of the symmetry energy.

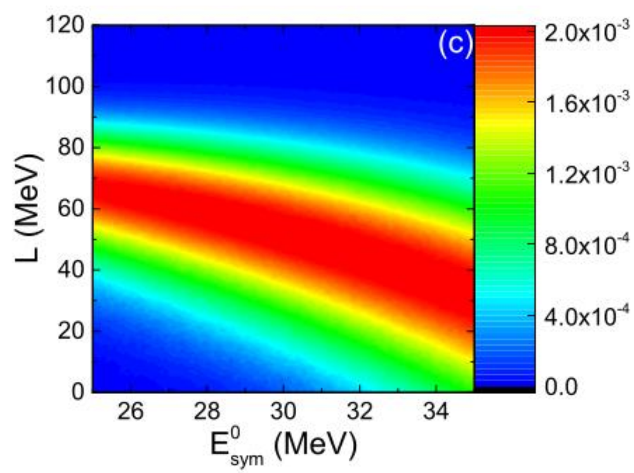

Jun Xu et al. PRC 102, 044316

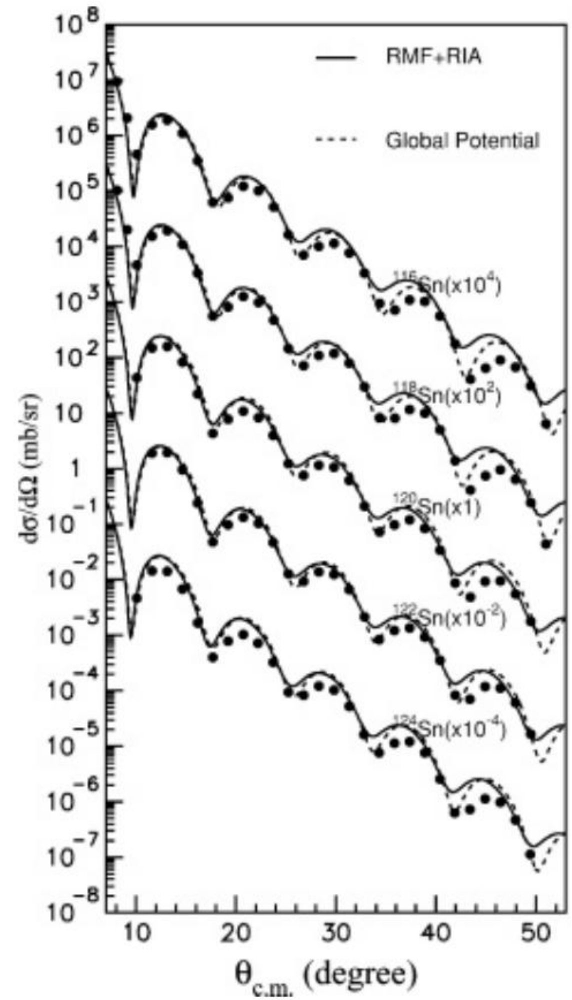

S. Terashima et al. PRC 77, 024317

Constraining the symmetry energy at $\rho \leq \rho_o$

Neutron skin thickness of neutron-rich nuclei

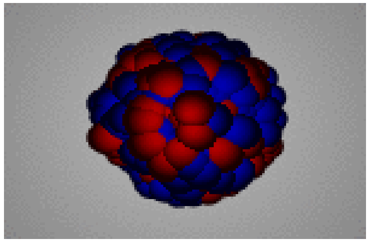

Electric dipole polarizability.

The dipole excitation induced in heavy neutron-rich nuclei traversing a Coulomb field generates a collective movement of protons against neutrons where the restoring force is governed by the symmetry energy.

State-of-the-art model calculations have proven a robust correlation between the measurable strength of the dipole excitation (α_D) and the density slope parameter of the symmetry energy (L). Measurements of the reaction ^{208}Pb(p,p') at RCNP (Osaka) provided a clear constraint of the value of L.

A. Tamii et al. PRL 107, 062502

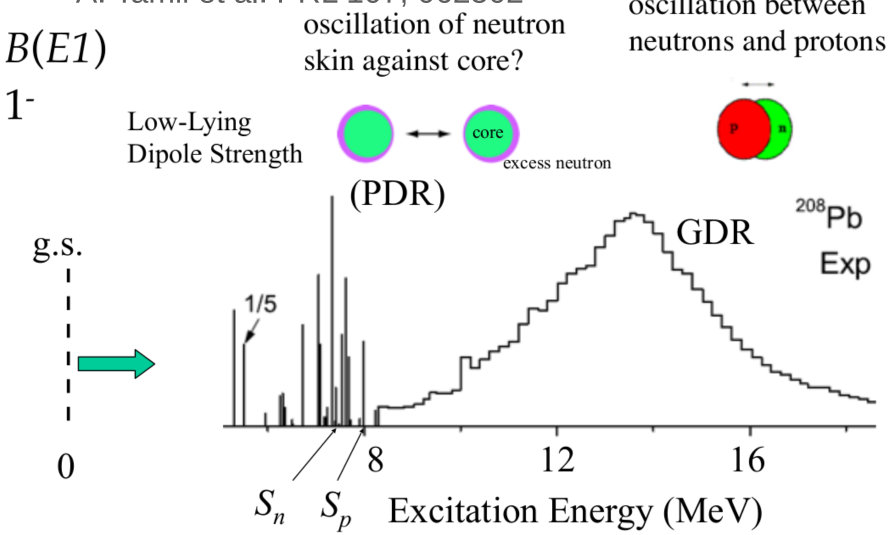

X. Roca-Maza et al. PRC 88, 024316

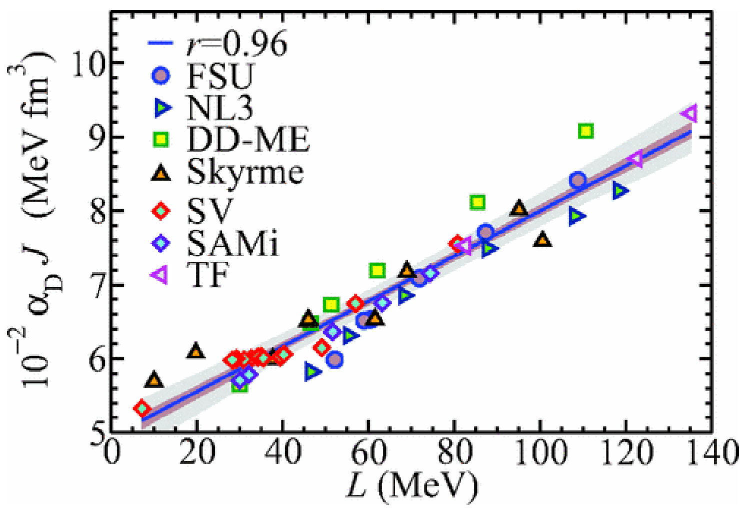

Constraining the symmetry energy at $\rho \leq \rho_o$

Neutron skin thickness of neutron-rich nuclei

Parity-violating electron scattering.

The interaction of relativistic electrons with nuclei can be mediated by the electromagnetic exchange of photons with protons, or the weak exchange of a Z_o boson with neutrons (the weak charge of the proton is very small). The weak interaction introduces a parity-violating term in the scattering amplitude that can be obtained from the measurement of the elastic electron-nucleus differential cross sections with electrons with different helicity.

$$A_{pv} = \frac{d\sigma^+/d\Omega - d\sigma^-/d\Omega}{d\sigma^+/d\Omega + d\sigma^-/d\Omega} \approx \frac{G_F q^2 F_W(q^2)}{2\pi\alpha\sqrt{2}F_{ch}(q^2)} \qquad F_W(q^2) = \int d^3r \frac{\sin(qr)}{qr}\rho_w(r)$$

Jefferson Lab, Virgina (USA)

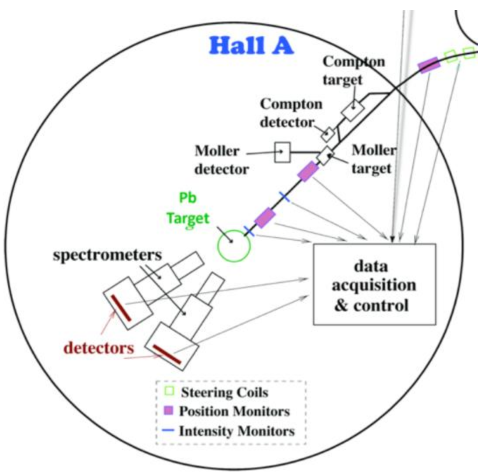

PREX experiment: high precision (~ 1%), almost model independent determination of the neutron-skin thickness in ^{208}Pb.

Constraining the symmetry energy at $\rho \leq \rho_o$

Heavy-ion collisions at intermediate energies

EOS is also an essential input in transport models used to describe heavy-ion collisions. One can then use suitable observables to constrain the symmetry energy at subsaturation densities.

In a neutron-rich environment, the symmetry potential tends to expel neutrons and attract protons, enhancing the yield ratios of ejected neutrons/protons and other isotopes while influencing their dependence on the ejected particle's momentum.

To gain sensitivity to the symmetric energy it was proposed to compare reactions with different isospin asymmetry as $^{124}Sn+^{124}Sn$, $^{112}Sn+^{112}Sn$, $^{124}Sn+^{112}Sn$, and then look to the emission of mirror clusters (n,p), (^{3}H,^{3}He), (^{7}Li,^{7}Be).

Describing measured isotopic ratios (R_i) or fragment flows with transport models, the parameters in the parabolic expansion of the symmetry energy could be constrained.

B. Tsang et al. PRL 102, 122701

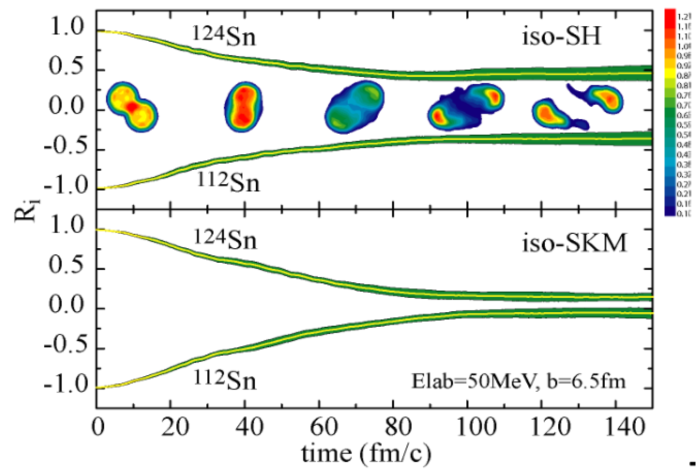

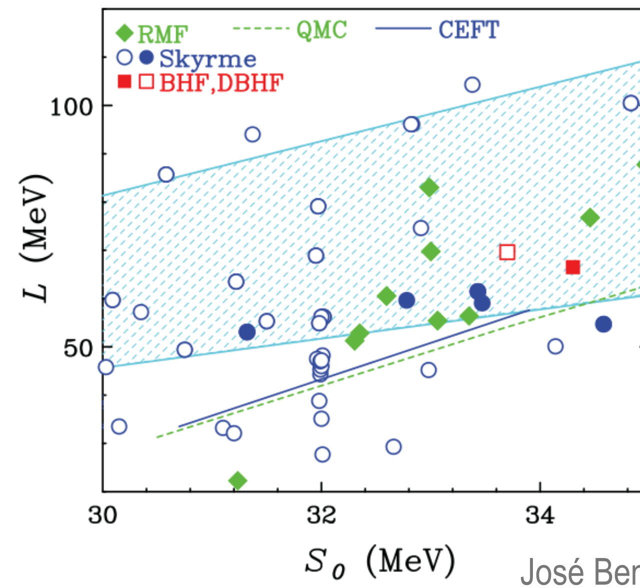

Constraining the symmetry energy at $\rho \leq \rho_0$

Combined analysis of terrestrial probes

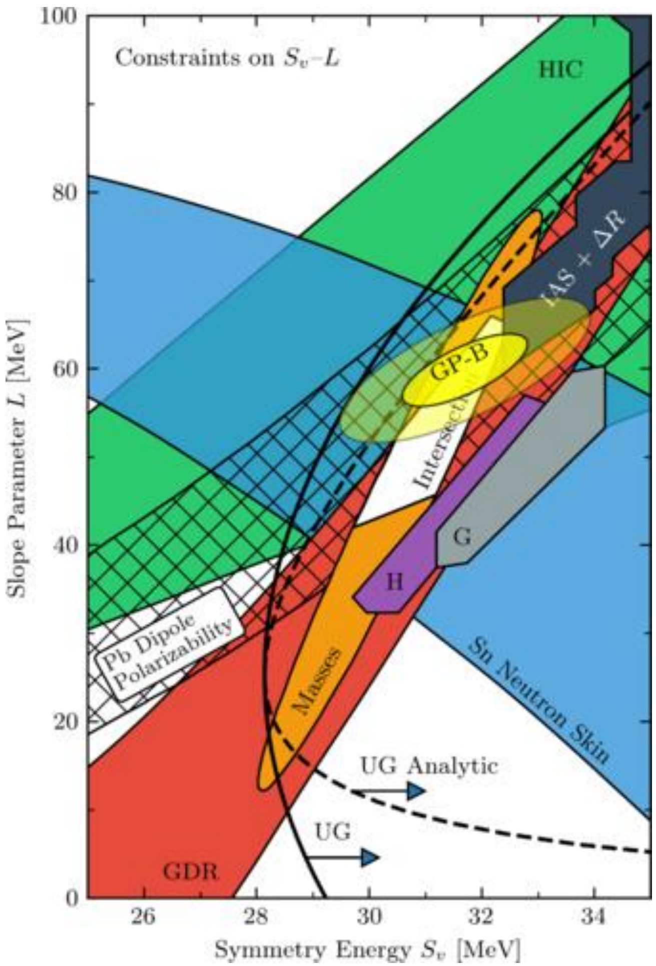

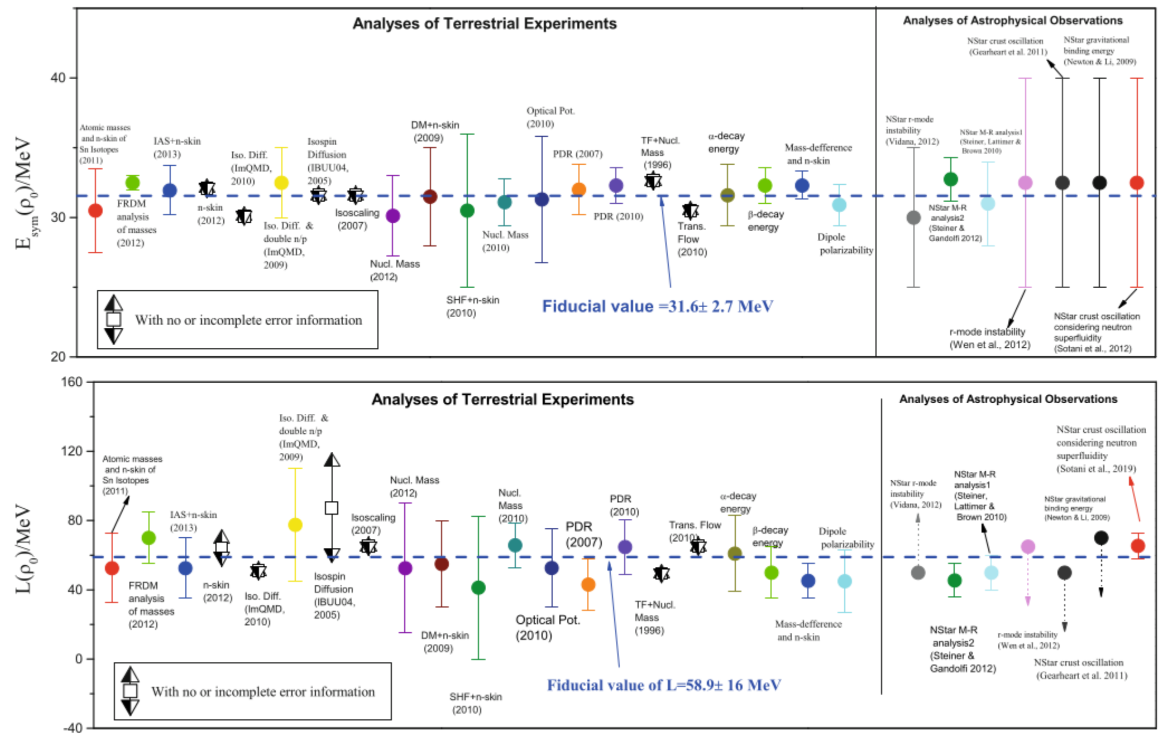

The combined analysis of the different terrestrial probes show a rather nice overlap providing the present fiducial values for the parameters describing the symmetry energy within the parabolic approximation.

$S_o = 31{,}6 \pm 2{,}7$ MeV $L = 58{,}9 \pm 16$ MeV

Constraining the symmetry energy at $\rho \leq \rho_o$

Recent results from PREX (parity-violating electron scattering)

PHYSICAL REVIEW LETTERS **126,** 172502 (2021)

Editors' Suggestion   Featured in Physics

Accurate Determination of the Neutron Skin Thickness of ^{208}Pb through Parity-Violation in Electron Scattering

D. Adhikari,[1] H. Albataineh,[2] D. Androic,[3] K. Aniol,[4] D. S. Armstrong,[5] T. Averett,[5] C. Ayerbe Gayoso,[5] S. Barcus,[6] V. Bellini,[7] R. S. Beminiwattha,[8] J. F. Benesch,[6] H. Bhatt,[9] D. Bhatta Pathak,[8] D. Bhetuwal,[9] B. Blaikie,[10] Q. Campagna,[5] A. Camsonne,[6] G. D. Cates,[11] Y. Chen,[8] C. Clarke,[12] J. C. Cornejo,[13] S. Covrig Dusa,[6] P. Datta,[14] A. Deshpande,[12,15] D. Dutta,[9] C. Feldman,[12] E. Fuchey,[14] C. Gal,[12,11,15] D. Gaskell,[6] T. Gautam,[16] M. Gericke,[10] C. Ghosh,[17,12] I. Halilovic,[10]

We report a precision measurement of the parity-violating asymmetry A_{PV} in the elastic scattering of longitudinally polarized electrons from ^{208}Pb. We measure $A_{PV} = 550 \pm 16(\text{stat}) \pm 8(\text{syst})$ parts per billion, leading to an extraction of the neutral weak form factor $F_W(Q^2 = 0.00616\ \text{GeV}^2) = 0.368 \pm 0.013$. Combined with our previous measurement, the extracted neutron skin thickness is $R_n - R_p = 0.283 \pm 0.071$ fm. The result also yields the first significant direct measurement of the interior weak density of ^{208}Pb: $\rho^0_W = -0.0796 \pm 0.0036(\text{exp}) \pm 0.0013(\text{theo})\ \text{fm}^{-3}$ leading to the interior baryon density $\rho^0_b = 0.1480 \pm 0.0036(\text{exp}) \pm 0.0013(\text{theo})\ \text{fm}^{-3}$. The measurement accurately constrains the density dependence of the symmetry energy of nuclear matter near saturation density, with implications for the size and composition of neutron stars.

Constraining the symmetry energy at $\rho \leq \rho_o$

Recent results from PREX-2 (parity-violating electron scattering)

Using the measured value for the ^{208}Pb skin thickness, the corresponding values for the parameters defining the symmetry energy are:

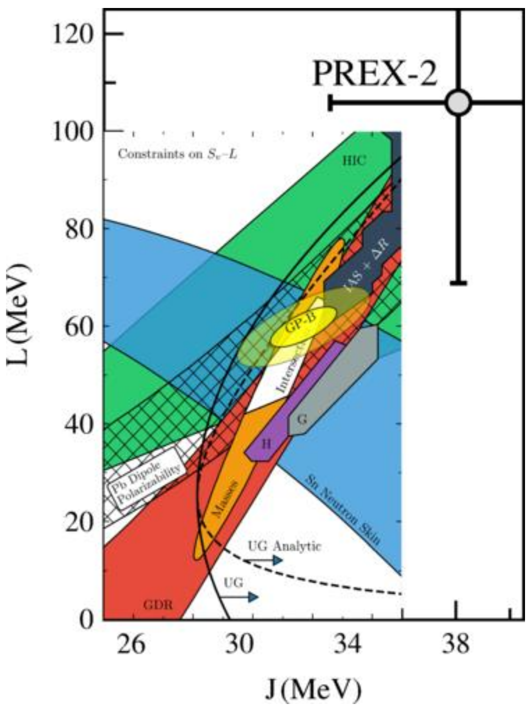

S_o/J = 38,1 ± 4,7 MeV

L = 106 ± 37 MeV

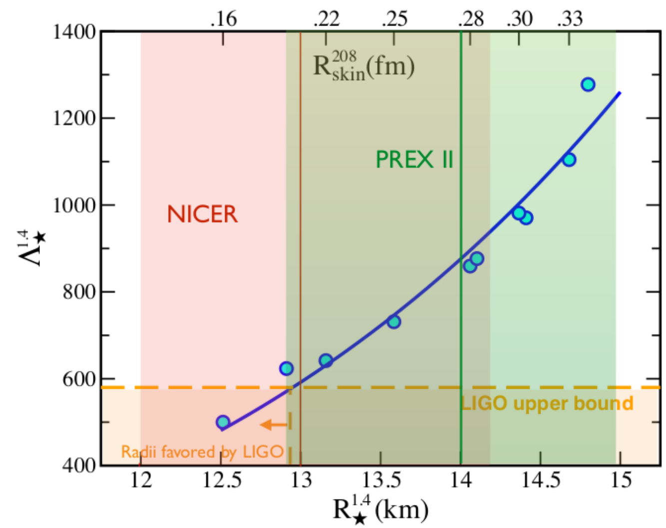

Comment of the reported results in Phys. Rev. Lett. 126, 172503:

``systematically overestimates current limits based on theoretical approaches and experimental measurements.´´

``The allowed region for the tidal deformability falls confortable within the $\Lambda_*^{1.4} \leq 800$ limit reported in the GW170817 discovery paper. Yet, the revised limit of $\Lambda_*^{1.4} \leq 580$ presents a more serious challenge.´´

Inner crust in neutron stars

Role of NN correlations

Because of the attractive nature of the NN force and the relative low temperatures in neutron stars, the formation of pairs of neutrons and protons in the inner crust and the core is expected. BCS theory provides the tools for describing this phenomenon.

Critical temperature for pairing

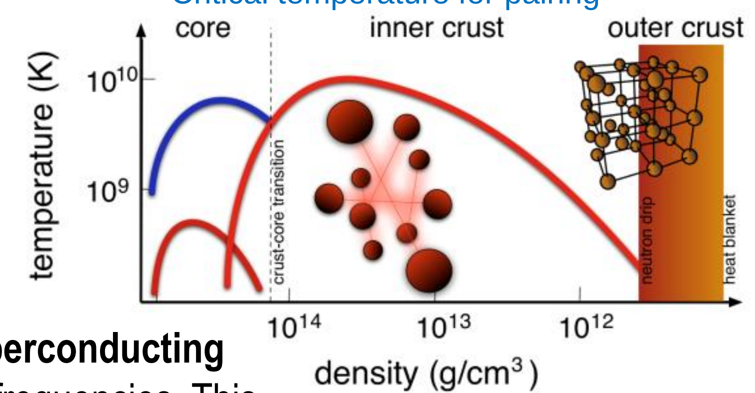

Evidences of the existence of these **superfluid** (neutrons) and **superconducting** (proton) phases are the observed **glitches** in neutron star rotation frequencies. This sudden increase in the star rotation frequency is explained by the coupling between the faster rotating superfluid in the star interior with the slower outer layers.

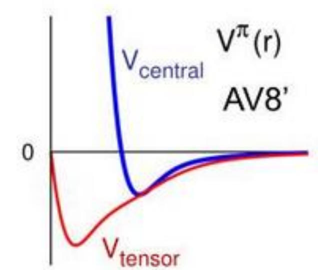

The repulsive central and tensor terms in the NN interaction also favors the formation of **short-range correlated NN pairs** with relative momenta above the Fermi momentum. The depletion of neutrons below the Fermi level may enhance the main cooling mechanism of neutron stars, the **direct URCA process**.

$$n \rightarrow p + e^{-} + \bar{\nu}_{e}$$

$$p + e^{-} \rightarrow n + \nu_{e}$$

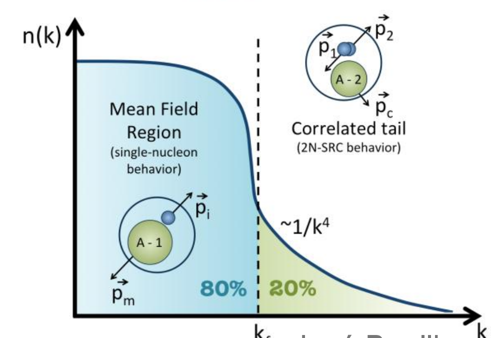

The large momentum of these nucleons, and the depopulation of states below the Fermi level, will also soften the EOS of neutron stars.

Inner crust in neutron stars

Experiments investigating short-range NN correlations

W.H. Dickhoff et al. PPNF 52, 377

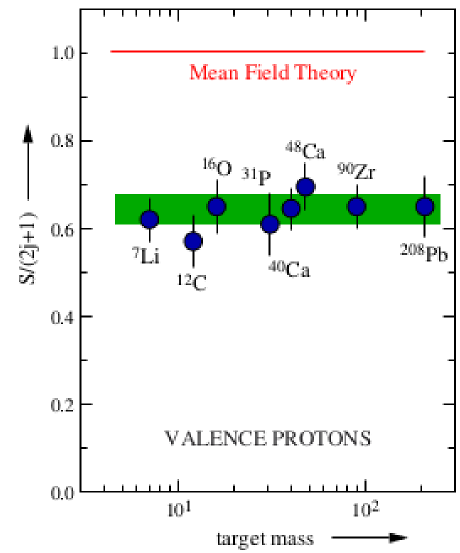

Experiments performed in the 80's at NIKHEF showed a 35% reduction in (*e,e'p*) reaction cross sections with respect to predictions based on the single-particle model. The missing cross section was explained as due long-range (LRC) and short-range (SRC) NN correlations.

Modern experiment by the CLAS collaboration at JLAB could identify SRC from the identification of high-momentum nucleons ($k>k_F$).in (*e,e'pp*) reactions. This measurements showed that around 20% of the nucleons form SRC pairs. Moreover, 90% of the SRC pairs are *n-p* while *n-n* and *p-p* SRC pairs represent 5% each.

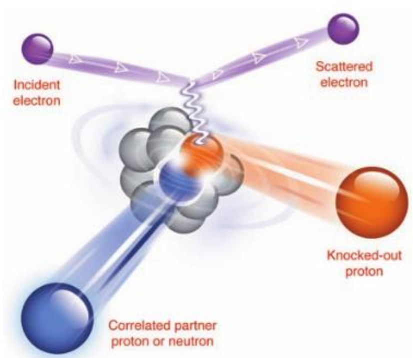

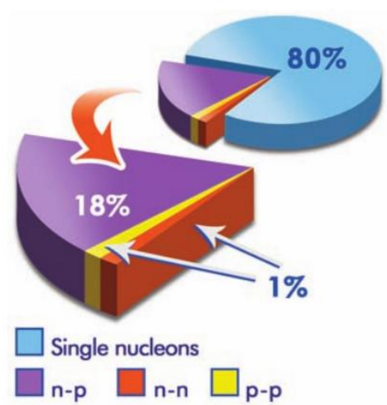

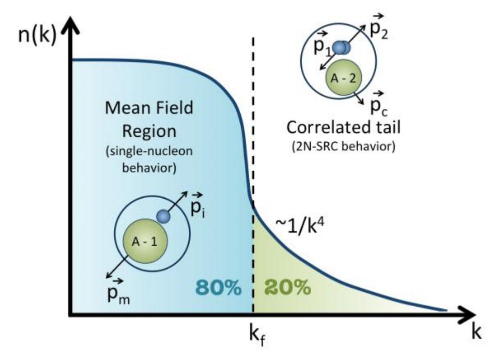

CLAS collaboration, Science 320, 1476

Experiments investigating short-range NN correlations

More recently, CLAS measurements also showed that due to the dominance of *n-p* SRC pairs, the relative number of protons with large momentum ($k>k_F$) increases with the neutron excess. This result would indicate that the few free protons present in the inner crust would have larger kinetic energies than expected, reducing the symmetry energy at high densities and softening the EOS.

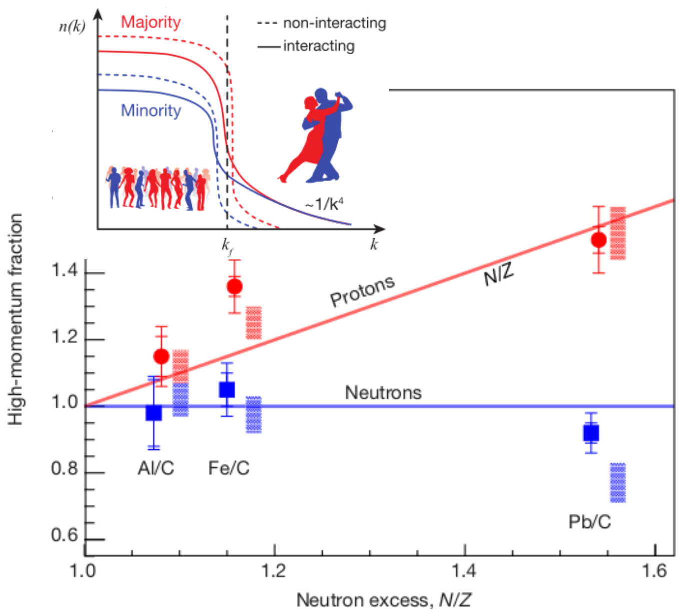

CLAS collaboration, Nature 560, 617

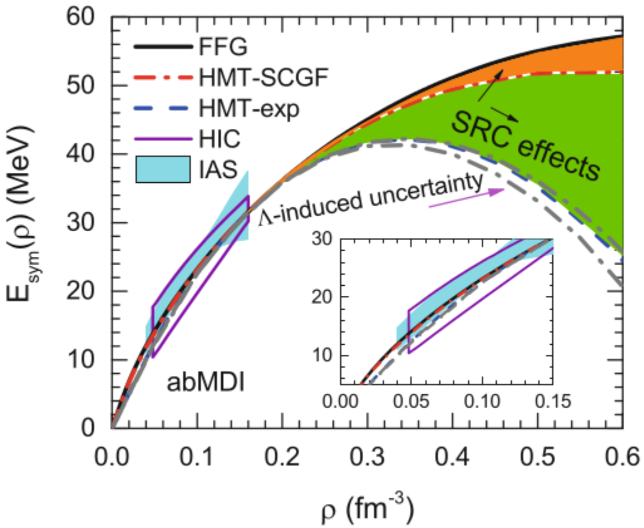

Bao-An Li, EPJA 55, 117

Core in neutron stars

Structure and composition

The core of neutron stars is characterized by matter at extreme densities ($\rho>\rho_0$) having a radial extension of around *10 km* and most of the mass of the star. Matter composition is expected to change drastically with density/depth.

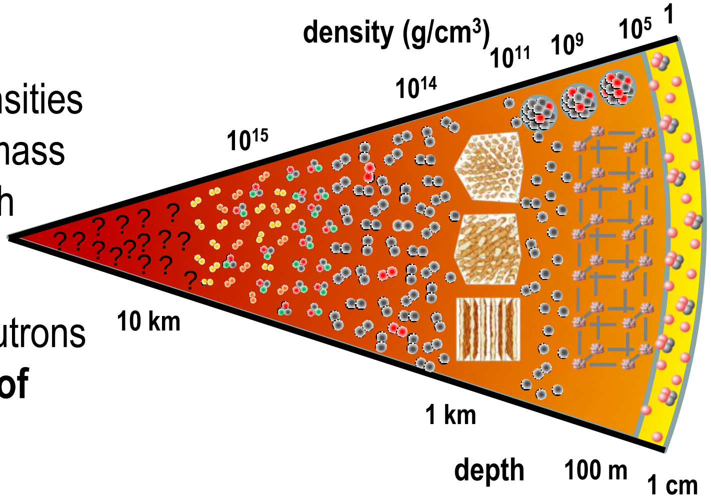

At $\rho_0 < \rho < 2\rho_0$ nuclear clusters dissolve into their constituents, neutrons and few protons (Y_e~*0,01*) coupled in pairs producing a **superfluid of neutrons,** and a **superconductors of protons**..

At $2\rho_0 < \rho < 3\rho_0$ the **electrons are transformed into muons** because the Fermi energy of the electrons is above the muon mass.

At $\rho >$ **2-3**ρ_0 the situation becomes rather uncertain. Models indicate the appearance of hyperons (Λ, Ξ) and baryon resonances (Δ). The highest densities may also produce kaon or pion condensates, or deconfined quark matter.

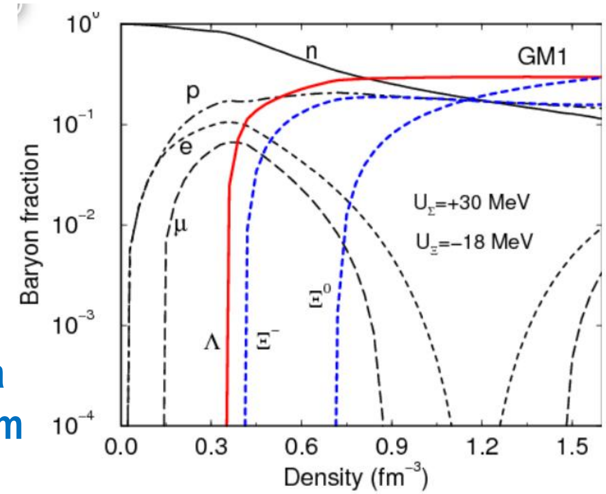

The main inputs for model calculations are the **symmetry energy at supra saturation density, NN correlations, YN and YY interactions, in-medium properties of hadrons,** …

Core in neutron stars

Symmetry energy at supra-saturation density ($\rho > \rho_o$)

Terrestrial experiments have constrained the symmetry energy at subsaturation to an acceptable level. The situation is however, very different at high densities both, from a theoretical and experimental point of view.

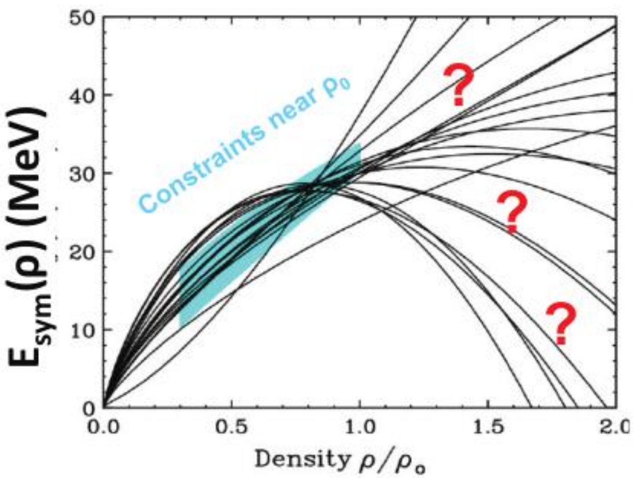

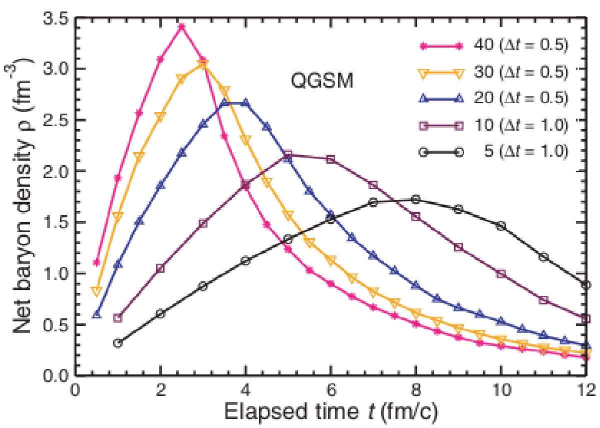

Nuclear matter at densities above saturation density can only be produced during the initial stage of heavy-ion collisions at relativistic energies.

According to transport model calculations, maximum compression of nuclear matter is achieved at energies around few A GeVs.

Observables sensitive to the reaction dynamics during the first compression phase have to be identified..

Measurements can only be related to the symmetry energy by using transport model calculations.

Core in neutron stars

Symmetry energy at supra saturation density ($\rho > \rho_o$)

The most relevant observables use to constraint the symmetry energy at supra-saturation density using heavy-ion collisions are:

- Ratios of isospin partners: n/p, 3He/t,….

- Pion or kaon production

- Elliptic flows

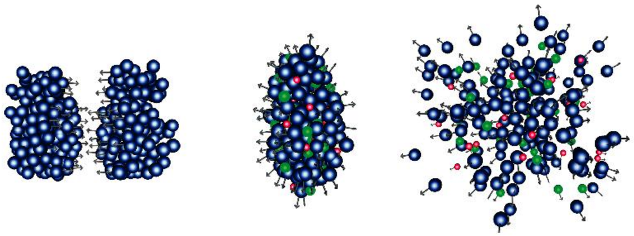

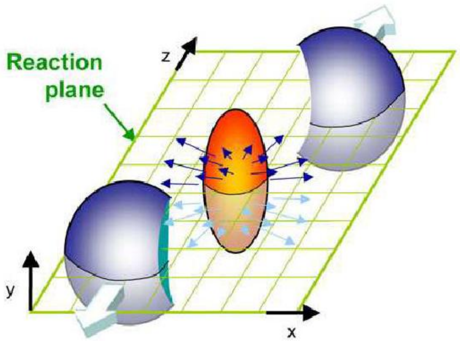

Those experiments require powerful heavy-ion accelerators and complex multi-detector systems: Despite some recent progress, a tighter constraint on the symmetry energy at high densities is challenging because the difficulties in precision experimental measurements, and strong model- and observable-dependent results.

Core in neutron stars

Symmetry energy at supra saturation density ($\rho > \rho_0$)

Measurements of the elliptic flows of neutrons and protons in ^{197}Au+^{197}Au collisions at *400A MeV* by the ASY-EOS and FOPI-LAND collaborations at GSI have provided the most relevant constraints of the symmetry energy at densities up to $3\rho_0$.

Additional constraints are provided by astronomic observations (massive neutron stars, tidal deformability,..).

FOPI experiment at GSI

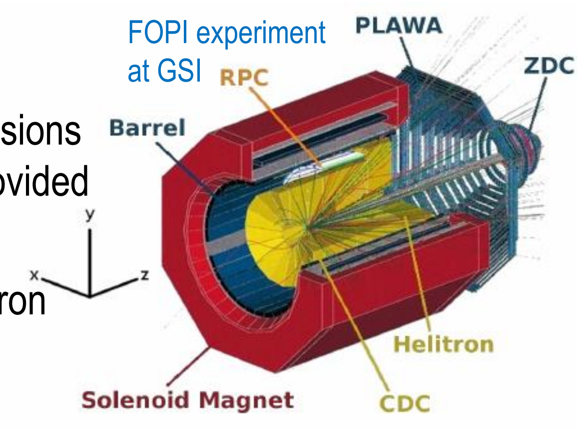

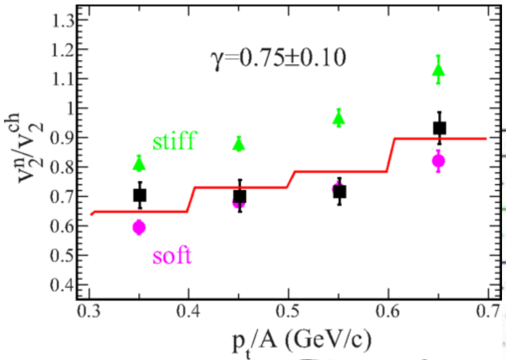

P. Russotto et al. PRC 94, 034608

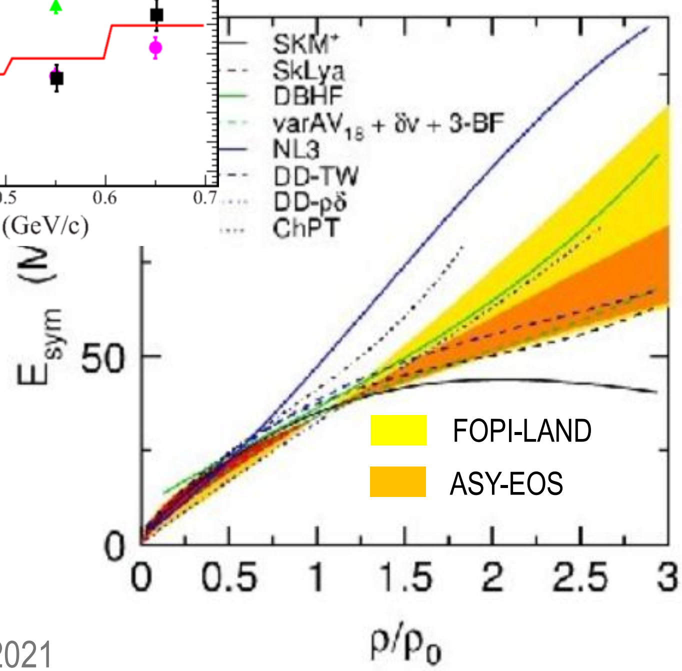

Y. Zhou et al., APJ 886, 52

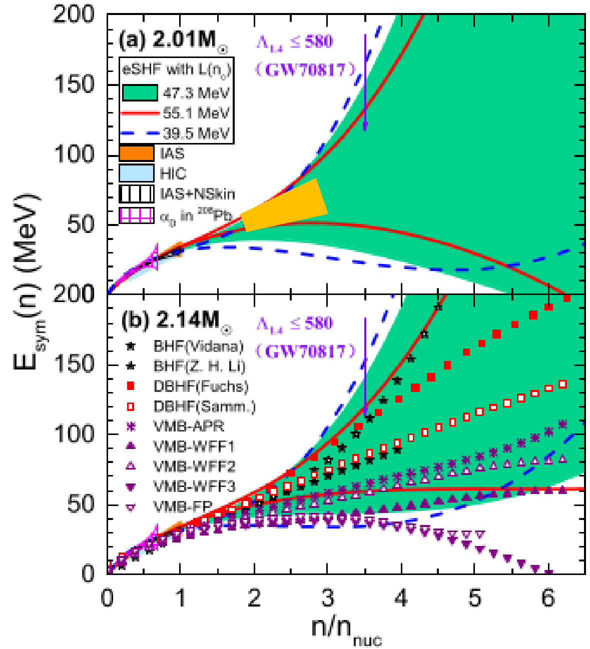

Core in neutron stars

Strange matter

Hyperons are expected to appear in the core of neutron stars at $\rho \sim (2\text{-}3)\rho_0$ when μ_N is large enough to make the conversion of *N* into *Y* energetically favorable. The most probable hyperon production reactions and the corresponding chemical potentials equilibrium conditions are:

$$n + e^- \rightarrow \Sigma^- + \nu_e \qquad \mu_\Sigma = \mu_n + \mu_e - \mu_\nu$$

$$n + n \rightarrow n + \Lambda \qquad \mu_\Lambda = \mu_n$$

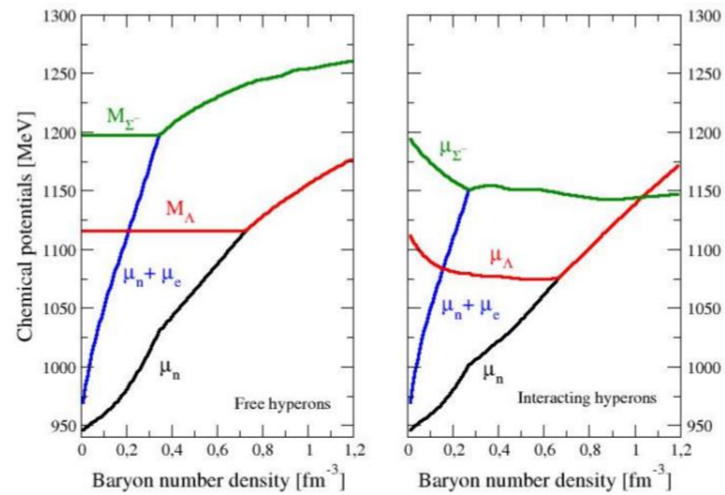

Hyperons soften EOS, and their inclusion does not allow to describe massive neutron stars $M \geq 2M_O$. The *YN* and *YY* interactions are however, poorly known.

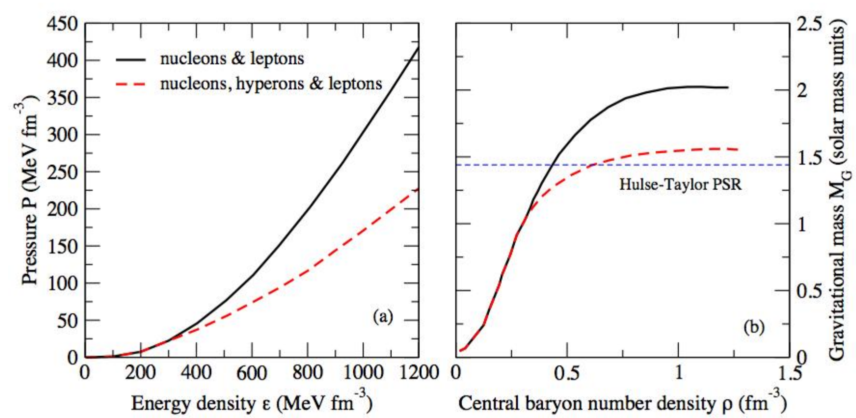

The accurate determination of the ***YN* and *YY* interactions** is of outmost importance.

Core in neutron stars

Experiments constraining YN and YY interactions

The main experimental techniques to produce and investigate hyperons are :

$K^- + N \rightarrow \Lambda + \pi^-$ **(BNL, Frascati, JPAC)** $\quad \pi^+ + N = \Lambda + K^+$ **(BNL, KEK, GSI)**

$e^- + N \rightarrow e^{-'} + K^+ + \Lambda$ **(JLAB, MAMI)** $\quad N + N = N + \Lambda + K^+$ **(CERN, GSI)**

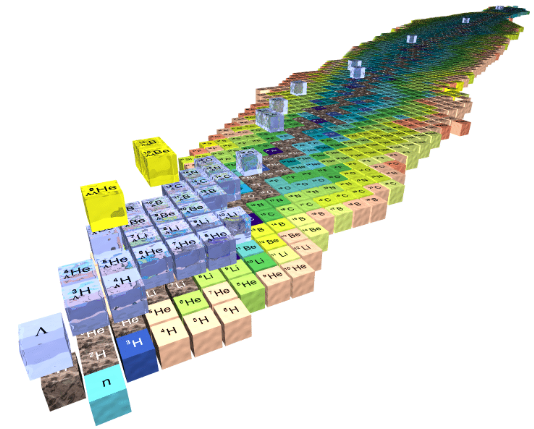

- **YN scattering**, although there are less than 40 data points compared with the more than 4000 for NN scattering at E_{lab}<350 MeV.

- **Hypernuclei production and mass determination.** Some 38 (*s*=-*1*) and 3 (*s*=-*2*) hypernuclei have been produced. $$M_{{}^A_\Lambda Z} - M_{{}^A Z} = B_{{}^A Z} - B_{{}^A_\Lambda Z} + M_\Lambda - M_N$$

- **Hypernuclei spectroscopy**. .

- **YN interaction from correlations.** Recently proposed at ALICE.

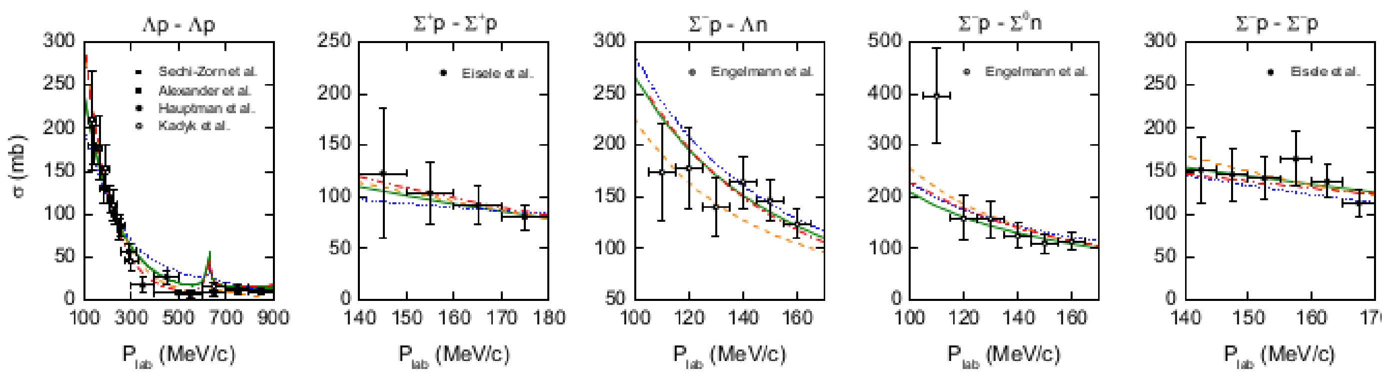

Core in neutron stars

Experiments constraining YN and YY interactions

YN interaction from p-Ω^- and p-Ξ^- correlations at ALICE

The correlation function between two hadrons (p-Ω^- and p-Ξ^-) with relative momentum $k^*=|p_1^*-p_2^*|/2$ produced in p-p collisions characterizes the interaction between these two hadrons.

$$C(k^*) = \int S(r^*)\left|\psi(k^*, r^*)\right|^2 d^3r^* = \xi(k^*)\,\frac{N_{same}(k^*)}{N_{mixed}(k^*)}$$

$$m_{\Lambda\pi} \to \Xi^- \to \Lambda + \pi^- \qquad m_{\Lambda K} \to \Omega^- \to \Lambda + K^-$$

The positive correlation functions indicates an attractive interaction that can not be explained by the Coulomb interaction (green curves).

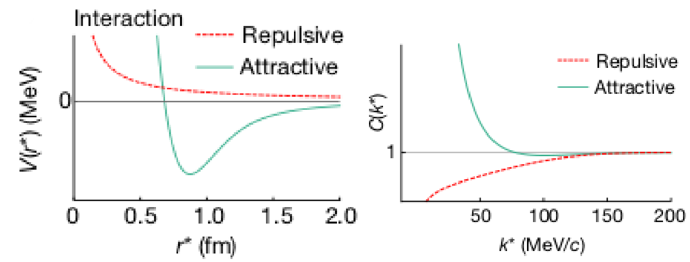

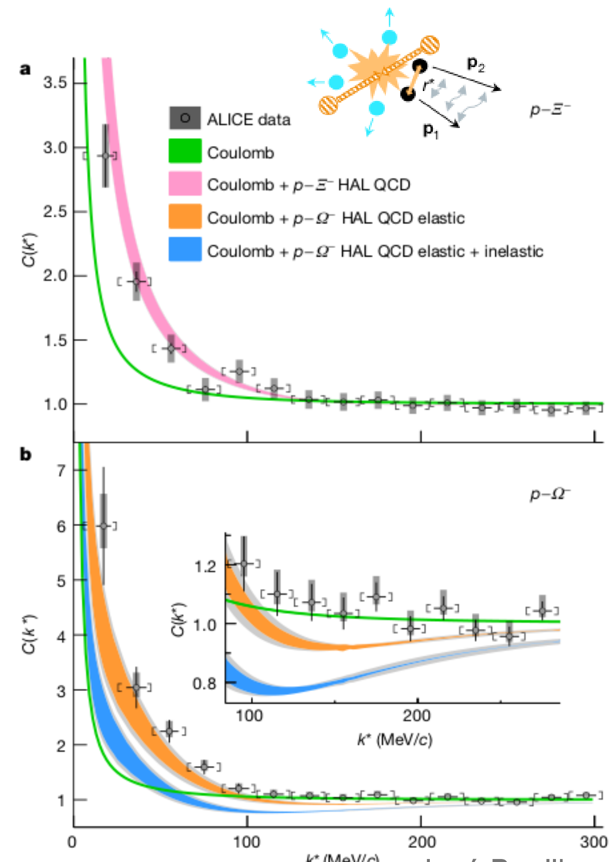

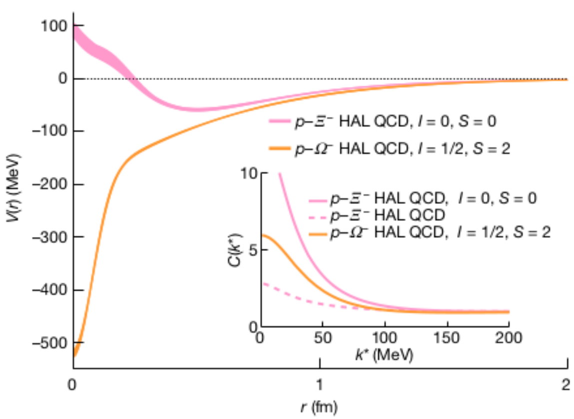

Lattice QCD calculations describing the measured correlation functions provide an accurate radial dependence of the strong interaction potentials..

ALICE collaboration, Nature 588, 232

Accreting neutron stars

Nucleosynthesis in X-ray binary systems

The matter accreted by the companion star (mostly hydrogen) generates a series of proton-induced thermonuclear reactions (rapid-proton capture) on the NS outer crust that modifies its composition creating heavy proton-rich nuclei.

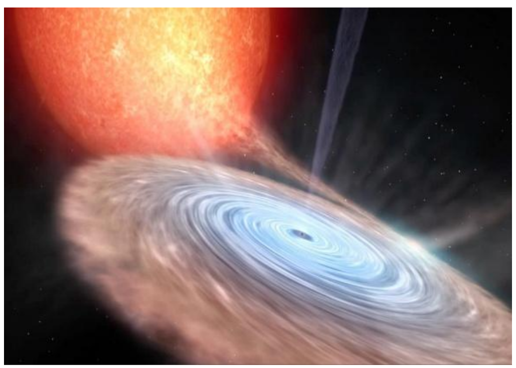

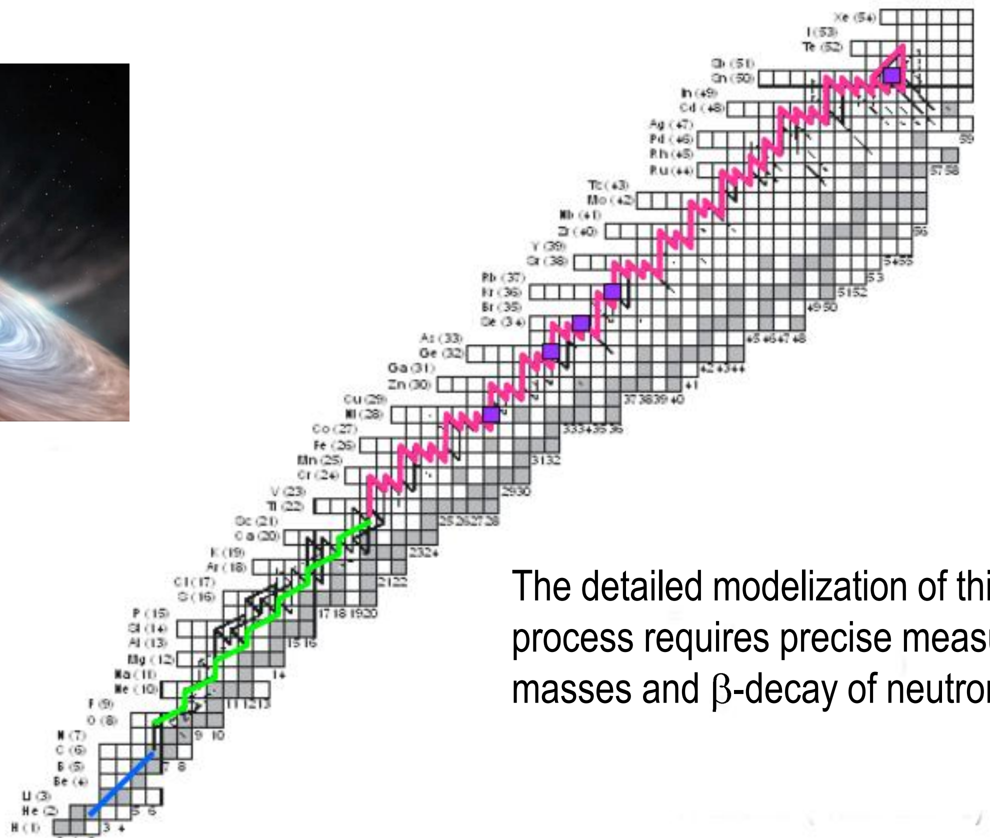

The detailed modelization of this nucleosynthesis process requires precise measurements on nuclear masses and β-decay of neutron-deficient nuclei.

Neutron star mergers

Nucleosynthesis in neutron star mergers

Neutron star mergers have been identified as a astrophysical scenario where r-process nucleosynthesis generates the heaviest chemical elements in the Universe. A detailed description of this process requires the production and investigation of heavy neutron-rich nuclei to validate nuclear models.

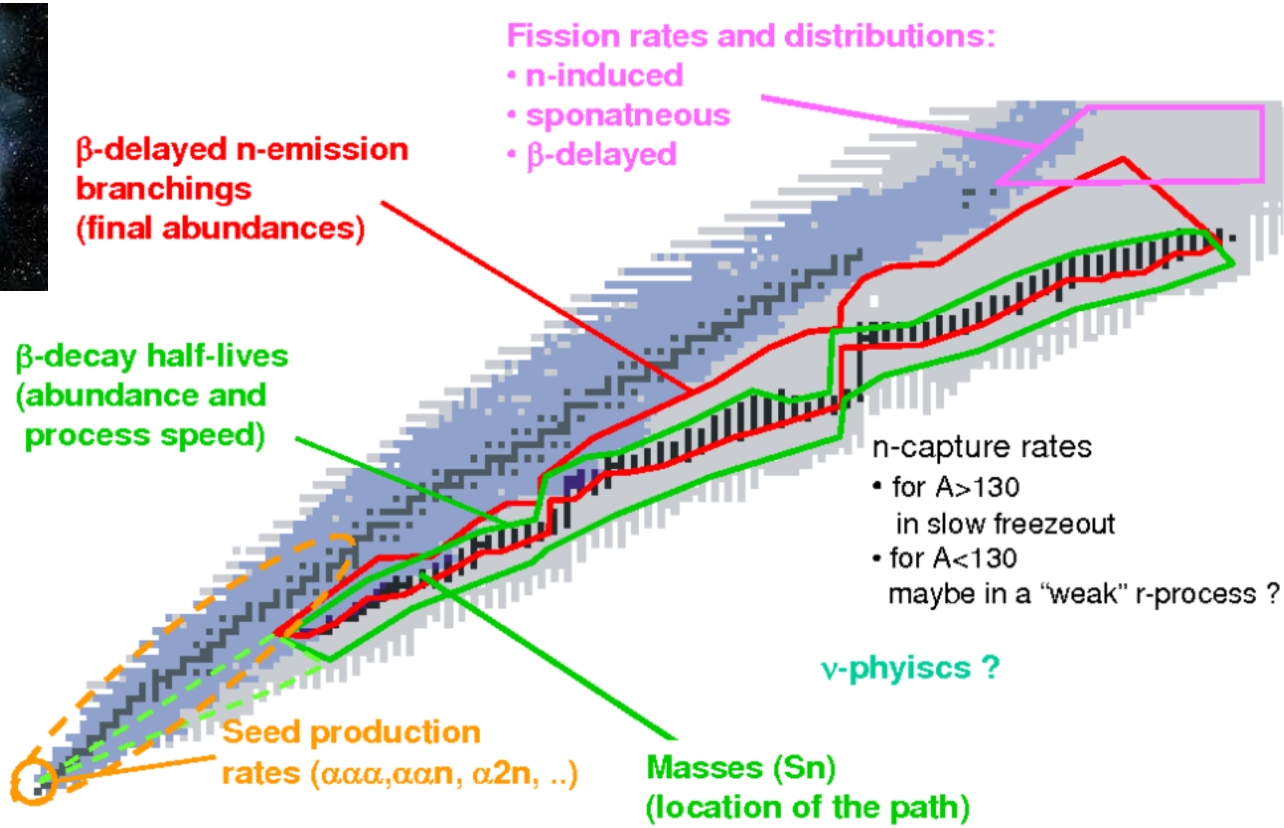

Terrestrial labs for the investigation of neutrons stars

More than twenty large scale accelerator facilities are producing inputs for the understanding of neutron stars.

Neutron stars in the laboratory

Facility for Antiproton and Ion Research in Darmstadt (Germany)

Neutron stars in the laboratory

Experiments with heavy-ion accelerators

Producing neutron star and binary neutron star merger matter

- ✓ Reactions induced by heavy ions
- ✓ Relativistic beams to produce dense nuclear matter (~2ρ_o) and excite subnucleonic degrees of freedom (nucleon resonances and hyperons)
- ✓ Radioactive Beams to produce neutron-rich nuclei

R^{3}B @ FAIR

Neutron stars in the laboratory

The R3B experiment

More than 4000 nuclear species at reach.

In particular the most neutron rich.

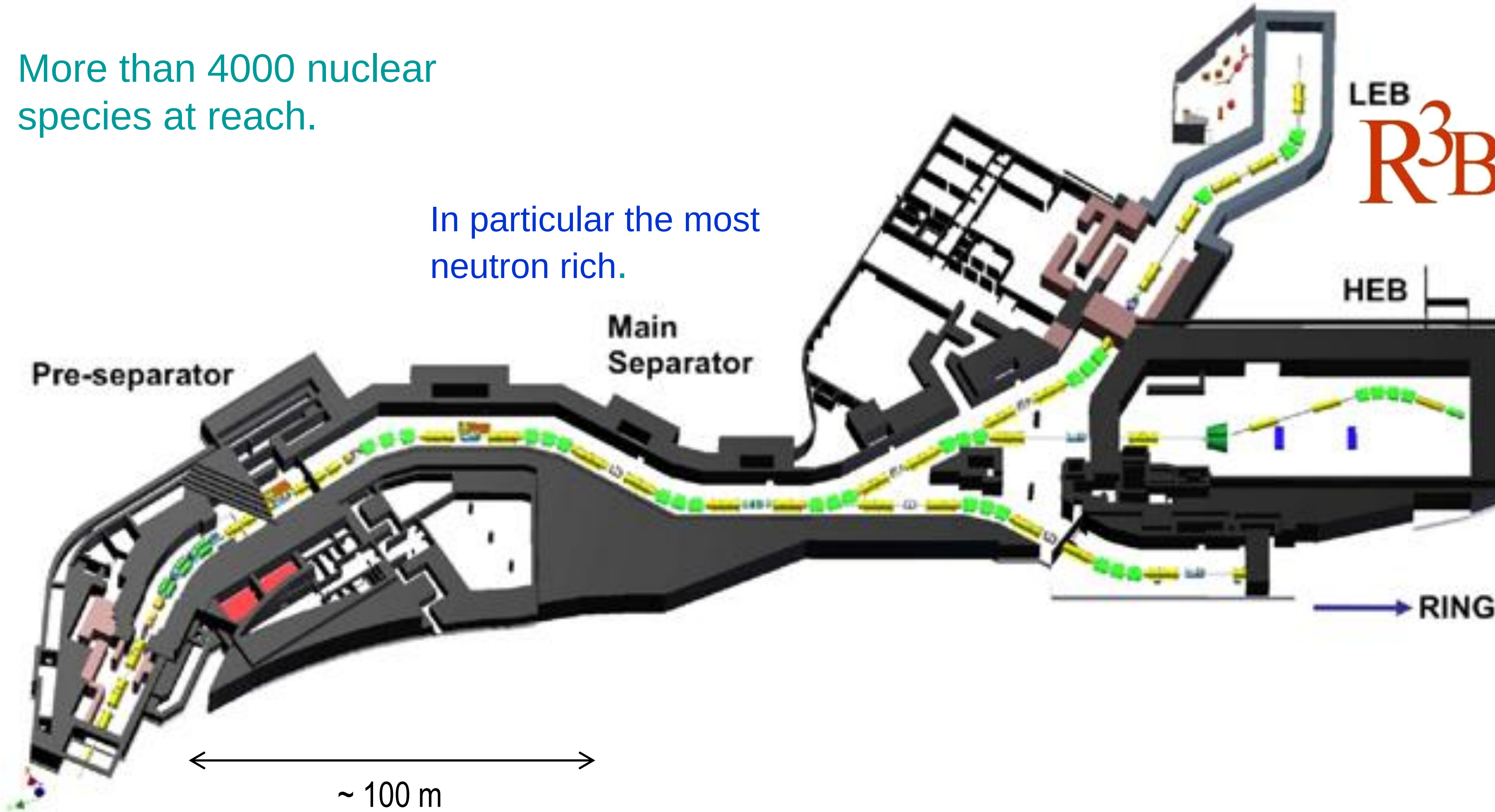

Neutron stars in the laboratory

The R3B experiment

Complete kinematics, fixed target experiments with relativistic radioactive beams

→ isotopic identification of projectile remnants: forward detectors

→ complete identification of γ-rays, nucleons and clusters: target area detectors

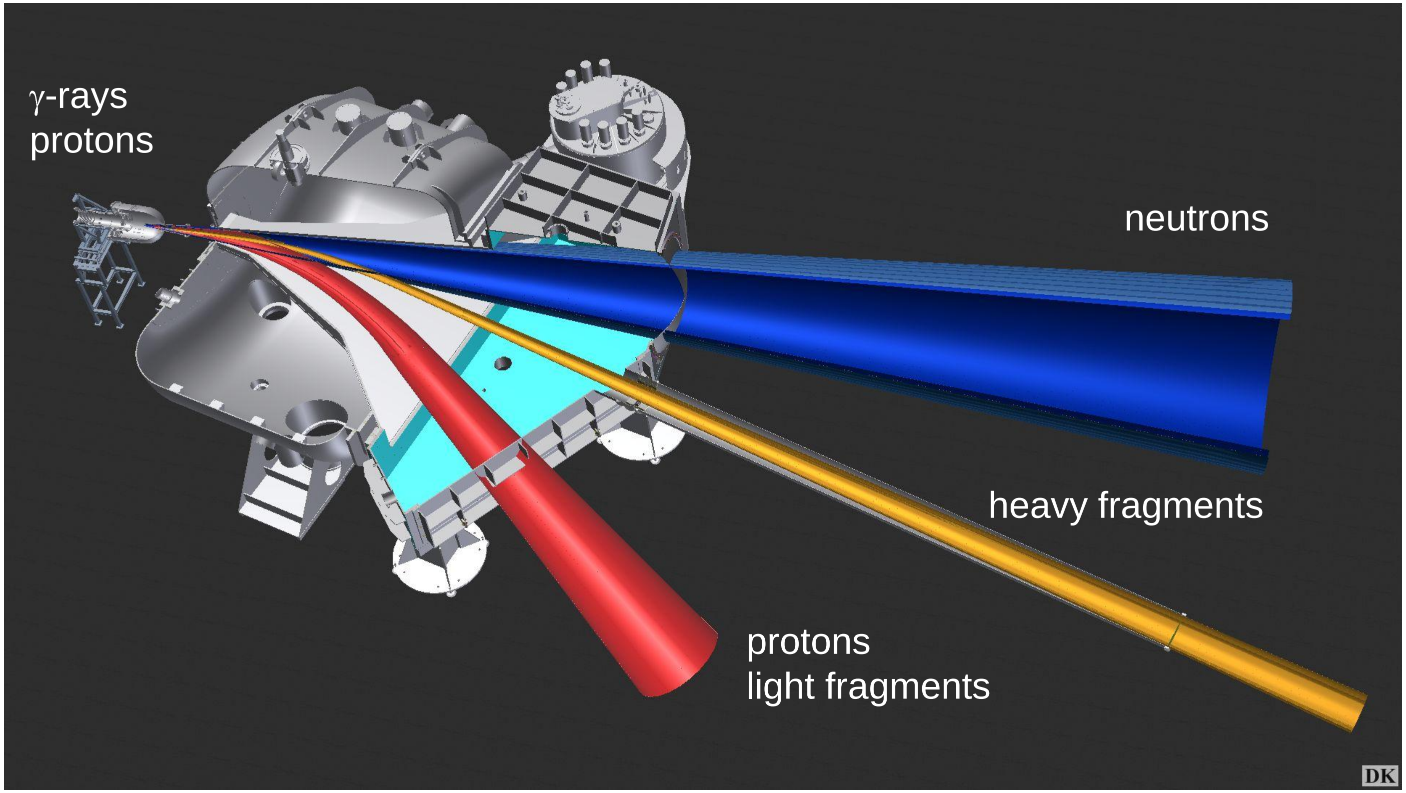

~ 250 scientists

GSI Helmholtzzentrum für Schwerionenforschung

Neutron stars in the laboratory

The R3B experiment

Neutron star matter

Neutron-rich nuclei

NN correlations

Equation of state

Hyper-nuclei

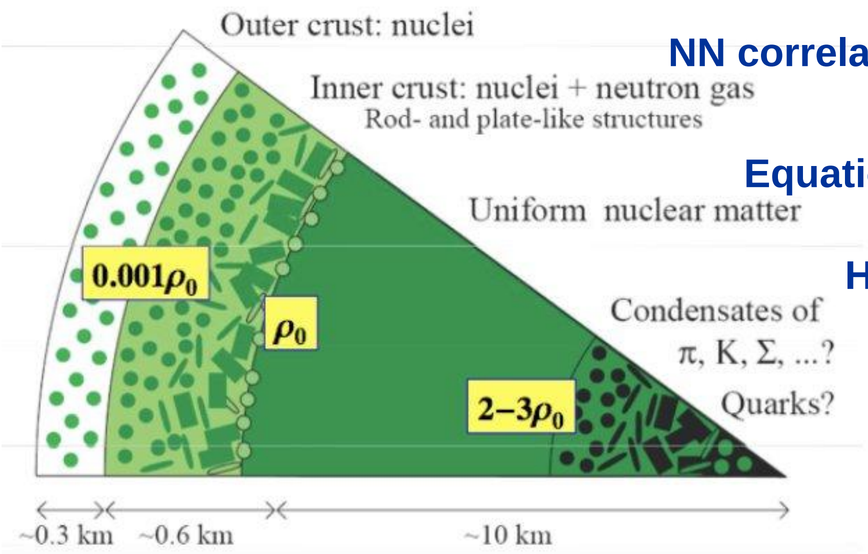

Neutron stars merger

The origin of the heaviest elements in the Universe

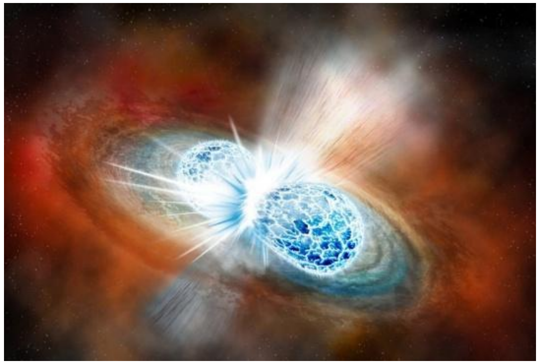

Conclusions

- ✓ The investigation of neutron stars requires a multi-disciplinary approach.
- ✓ Experimental nuclear physics is providing inputs to improve nuclear models describing the structure and composition of nucleon stars.
- ✓ Next generation facilities delivering beams of neutron-rich nuclei at relativistic energies are expected to represent a real break-through on the investigation of neutron stars in the lab.

Structure of neutron stars

5.5 Neutron star crust

A quantitative description of the neutron star crust requires a reliable EOS. The constraint of the symmetry energy seems mandatory.

$$P(\rho,\beta) = \frac{\rho^2}{3\rho_o}\left(L\beta^2 + \left(K_o + K_{sym}\beta^2\right)\frac{\rho-\rho_o}{3\rho_o} + \cdots\right)$$

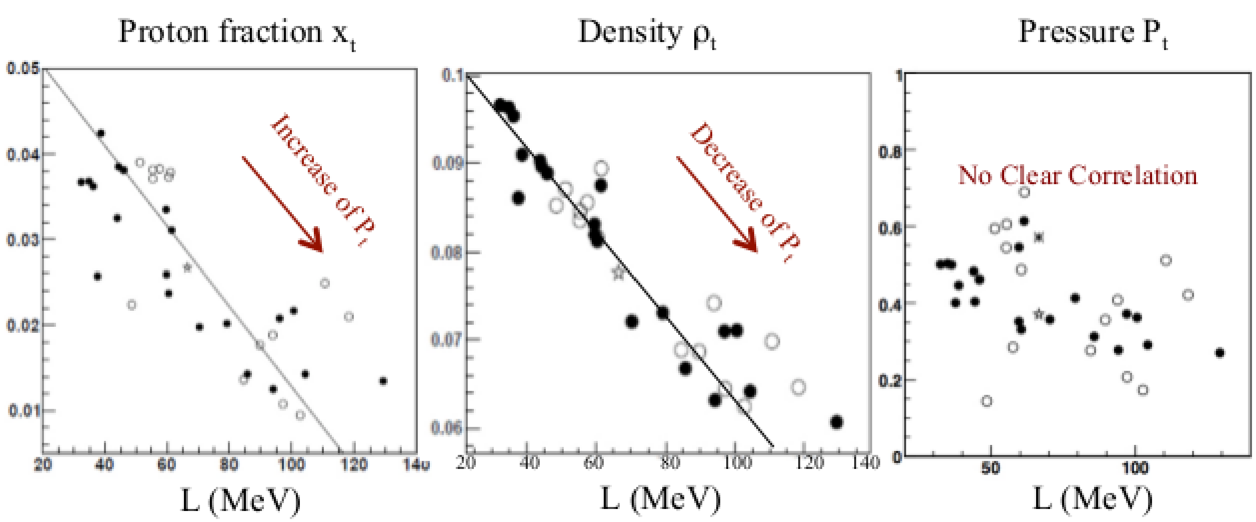

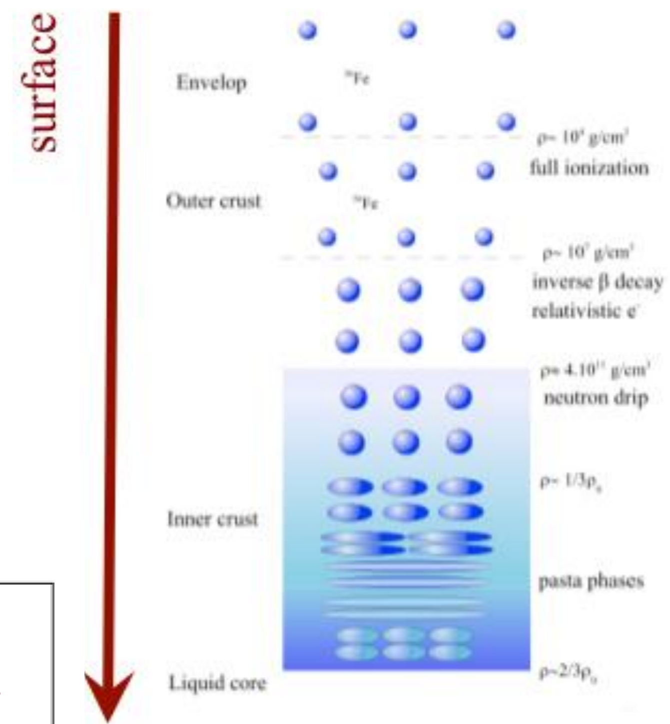

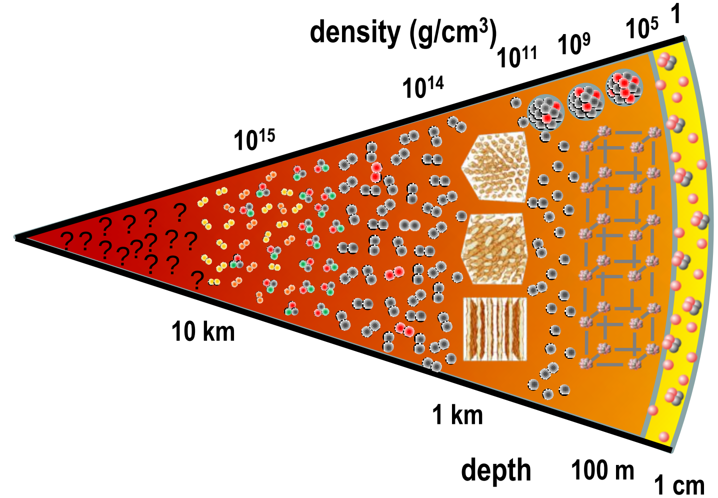

density (g/cm^3)
10^{15}
10^{14}
10^{11}
10^{9}
10^{5}
1
10 km
1 km
depth
100 m
1 cm

6.2 Nucleon resonances in the neutron star core

In a similar way to hyperons, nucleon resonances as the Δ isobars may appear in the core of neutron stars above a given ρ^{cri}.

$$\Delta^{++} + n \leftrightarrow p + p \qquad \mu_{\Delta^{++}} = 2\mu_p - \mu_n$$

$$\Delta^{+} + n \leftrightarrow n + p \qquad \mu_{\Delta^{+}} = \mu_p$$

$$\Delta^{0} + p \leftrightarrow n + p \qquad \mu_{\Delta^{0}} = \mu_n$$

$$\Delta^{-} + p \leftrightarrow n + n \qquad \mu_{\Delta^{-}} = 2\mu_n - \mu_p$$

$$\rightarrow \quad {\rho^{cri}}_{\Delta^-} < {\rho^{cri}}_{\Delta^0} < {\rho^{cri}}_{\Delta^+} < {\rho^{cri}}_{\Delta^{++}}$$

Nucleon resonances also soften the equation of state.

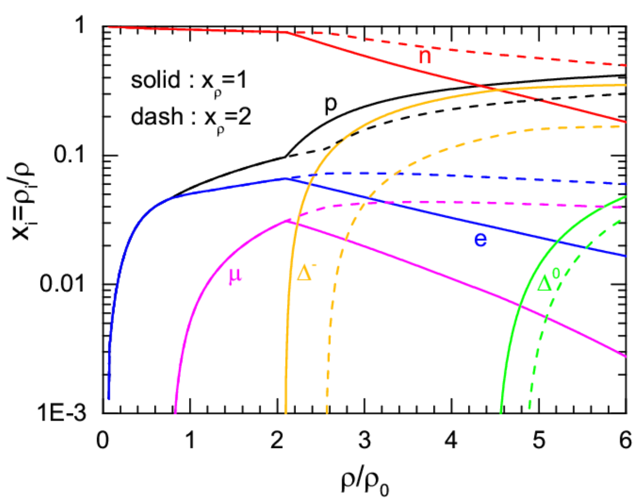

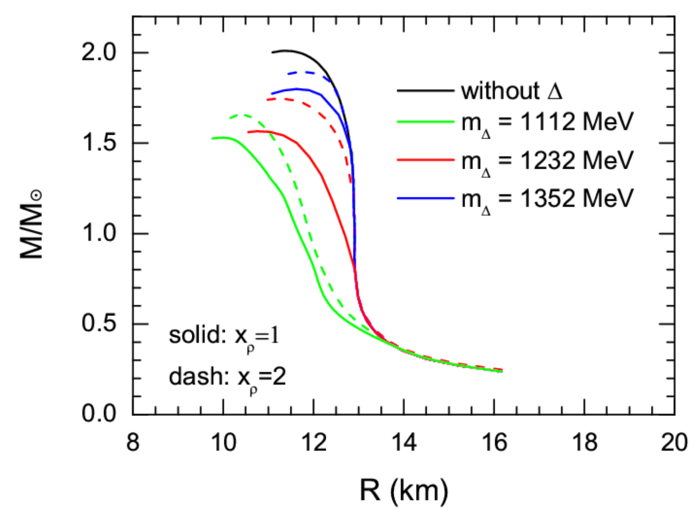

Neutron stars in the laboratory

Facility for Antiproton and Ion Research